



TECH BRIEFS

NATIONAL AERONAUTICS AND SPACE ADMINISTRATION

-  **Technology Focus**
-  **Electronics/Computers**
-  **Software**
-  **Materials**
-  **Mechanics/Machinery**
-  **Manufacturing**
-  **Bio-Medical**
-  **Physical Sciences**
-  **Information Sciences**
-  **Books and Reports**

INTRODUCTION

Tech Briefs are short announcements of innovations originating from research and development activities of the National Aeronautics and Space Administration. They emphasize information considered likely to be transferable across industrial, regional, or disciplinary lines and are issued to encourage commercial application.

Additional Information on NASA Tech Briefs and TSPs

Additional information announced herein may be obtained from the NASA Technical Reports Server: <http://ntrs.nasa.gov>.

Please reference the control numbers appearing at the end of each Tech Brief. Information on NASA's Innovative Partnerships Program (IPP), its documents, and services is available on the World Wide Web at <http://www.ipp.nasa.gov>.

Innovative Partnerships Offices are located at NASA field centers to provide technology-transfer access to industrial users. Inquiries can be made by contacting NASA field centers listed below.

NASA Field Centers and Program Offices

Ames Research Center

David Morse
(650) 604-4724
david.r.morse@nasa.gov

Dryden Flight Research Center

Ron Young
(661) 276-3741
ronald.m.young@nasa.gov

Glenn Research Center

Kimberly A. Dalgleish-Miller
(216) 433-8047
kimberly.a.dalgleish@nasa.gov

Goddard Space Flight Center

Nona Cheeks
(301) 286-5810
nona.k.cheeks@nasa.gov

Jet Propulsion Laboratory

Indrani Graczyk
(818) 354-2241
indrani.graczyk@jpl.nasa.gov

Johnson Space Center

John E. James
(281) 483-3809
john.e.james@nasa.gov

Kennedy Space Center

David R. Makufka
(321) 867-6227
david.r.makufka@nasa.gov

Langley Research Center

Michelle Ferebee
(757) 864-5617
michelle.t.ferebee@nasa.gov

Marshall Space Flight Center

Terry L. Taylor
(256) 544-5916
terry.taylor@nasa.gov

Stennis Space Center

Ramona Travis
(228) 688-3832
ramona.e.travis@ssc.nasa.gov

NASA Headquarters

Daniel Lockney,
Technology Transfer Program Executive
(202) 358-2037
daniel.p.lockney@nasa.gov

Small Business Innovation Research (SBIR) & Small Business Technology Transfer (STTR) Programs

Rich Leshner, Program Executive
(202) 358-4920
rleshner@nasa.gov



TECH BRIEFS

NATIONAL AERONAUTICS AND SPACE ADMINISTRATION

5 Technology Focus: Test & Measurement

- 5 Beat-to-Beat Blood Pressure Monitor
- 5 Measurement Techniques for Clock Jitter
- 6 Lightweight, Miniature Inertial Measurement System
- 6 Optical Density Analysis of X-Rays Utilizing Calibration Tooling to Estimate Thickness of Parts
- 7 Fuel Cell/Electrochemical Cell Voltage Monitor
- 7 Anomaly Detection Techniques With Real Test Data From a Spinning Turbine Engine-Like Rotor
- 8 Measuring Air Leaks Into the Vacuum Space of Large Liquid Hydrogen Tanks
- 8 Antenna Calibration and Measurement Equipment

11 Manufacturing & Prototyping

- 11 Glass Solder Approach for Robust, Low-Loss, Fiber-to-Waveguide Coupling
- 11 Lightweight Metal Matrix Composite Segmented for Manufacturing High-Precision Mirrors
- 12 Plasma Treatment To Remove Carbon From Indium UV Filters

15 Electronics/Computers

- 15 Telerobotics Workstation (TRWS) for Deep Space Habitats
- 16 Single-Pole Double-Throw MMIC Switches for a Microwave Radiometer
- 16 On Shaft Data Acquisition System (OSDAS)
- 17 ASIC Readout Circuit Architecture for Large Geiger Photodiode Arrays
- 18 Flexible Architecture for FPGAs in Embedded Systems

19 Materials & Coatings

- 19 Polyurea-Based Aerogel Monoliths and Composites
- 19 Resin-Impregnated Carbon Ablator: A New Ablative Material for Hyperbolic Entry Speeds
- 20 Self-Cleaning Particulate Prefilter Media

23 Mechanics/Machinery

- 23 Modular, Rapid Propellant Loading System/Cryogenic Testbed
- 23 Compact, Low-Force, Low-Noise Linear Actuator
- 24 Loop Heat Pipe With Thermal Control Valve as a Variable Thermal Link
- 25 Process for Measuring Over-Center Distances

27 Bio-Medical

- 27 Hands-Free Transcranial Color Doppler Probe
- 27 Improving Balance Function Using Low Levels of Electrical Stimulation of the Balance Organs
- 28 Developing Physiologic Models for Emergency Medical Procedures Under Microgravity
- 28 PMA-Linked Fluorescence for Rapid Detection of Viable Bacterial Endospores
- 29 Portable Intravenous Fluid Production Device for Ground Use
- 30 Adaptation of a Filter Assembly to Assess Microbial Bioburden of Pressurant Within a Propulsion System

31 Physical Sciences

- 31 Multiplexed Force and Deflection Sensing Shell Membranes for Robotic Manipulators
- 31 Whispering Gallery Mode Optomechanical Resonator
- 32 Vision-Aided Autonomous Landing and Ingress of Micro Aerial Vehicles
- 33 Self-Sealing Wet Chemistry Cell for Field Analysis

35 Information Sciences

- 35 General MACOS Interface for Modeling and Analysis for Controlled Optical Systems

37 Books & Reports

- 37 Mars Technology Rover with Arm-Mounted Percussive Coring Tool, Microimager, and Sample-Handling Encapsulation Containerization Subsystem
- 37 Fault-Tolerant, Real-Time, Multi-Core Computer System

39 Software

- 39 Water Detection Based on Object Reflections
- 40 SATPLOT for Analysis of SECCHI Heliospheric Imager Data
- 40 Plug-in Plan Tool v3.0.3.1
- 41 Frequency Correction for MIRO Chirp Transformation Spectroscopy Spectrum
- 41 Nonlinear Estimation Approach to Real-Time Georegistration from Aerial Images
- 42 Optimal Force Control of Vibro-Impact Systems for Autonomous Drilling Applications
- 43 Low-Cost Telemetry System for Small/Micro Satellites
- 43 Operator Interface and Control Software for the Reconfigurable Surface System Tri-ATHLETE

This document was prepared under the sponsorship of the National Aeronautics and Space Administration. Neither the United States Government nor any person acting on behalf of the United States Government assumes any liability resulting from the use of the information contained in this document, or warrants that such use will be free from privately owned rights.

44	Algorithms for Determining Physical Responses of Structures Under Load	50	Large Terrain Continuous Level of Detail 3D Visualization Tool
45	Mission Analysis, Operations, and Navigation Toolkit Environment (Monte) Version 040	50	SE-FIT
45	Autonomous Rover Traverse and Precise Arm Placement on Remotely Designated Targets	51	Scalable Integrated Multi-Mission Support System Simulator Release 3.0
46	Computing Radiative Transfer in a 3D Medium	51	Mars Express Forward Link Capabilities for the Mars Relay Operations Service (MaROS)
46	Architectural Implementation of NASA Space Telecommunications Radio System Specification	52	FERMI/GLAST Integrated Trending and Plotting System Release 5.0
46	Journal and Wave Bearing Impedance Calculation Software	52	Where's My Data — WMD
47	Scalable Integrated Multi-Mission Support System (SIMSS) Simulator Release 2.0 for GMSEC	53	Tiled WMS/KML Server V2
47	Policy-Based Negotiation Engine for Cross-Domain Interoperability	53	CometQuest: A Rosetta Adventure
48	Linked-List-Based Multibody Dynamics (MBDyn) Engine	53	Dig Hazard Assessment Using a Stereo Pair of Cameras
48	Multi-Mission Power Analysis Tool (MMPAT) Version 3	54	High-Performance Modeling and Simulation of Anchoring in Granular Media for NEO Applications
49	Jupiter Environment Tool	55	Mobile Multi-System Overview
49	Jet and Tropopause Products for Analysis and Characterization (JETPAC)	55	Leveraging Cloud Computing to Improve Storage Durability, Availability, and Cost for MER Maestro
49	WGM Temperature Tracker	56	WMS Server 2.0
		56	I-FORCAST: Rapid Flight Planning Tool
		57	Earth-Science Data Co-Locating Tool
		57	Ascent/Descent Software

This document was prepared under the sponsorship of the National Aeronautics and Space Administration. Neither the United States Government nor any person acting on behalf of the United States Government assumes any liability resulting from the use of the information contained in this document, or warrants that such use will be free from privately owned rights.



Beat-to-Beat Blood Pressure Monitor

This invention is applicable to all segments of the blood pressure monitoring market, including ambulatory, home-based, and high-acuity monitoring.

Lyndon B. Johnson Space Center, Houston, Texas

This device provides non-invasive beat-to-beat blood pressure measurements and can be worn over the upper arm for prolonged durations. Phase and waveform analyses are performed on filtered proximal and distal photoplethysmographic (PPG) waveforms obtained from the brachial artery. The phase analysis is used primarily for the computation of the mean arterial pressure, while the waveform analysis is used primarily to obtain the pulse pressure. Real-time compliance estimate is used to refine both the mean arterial and pulse pressures to provide the beat-to-beat blood pressure measurement.

This wearable physiological monitor can be used to continuously observe the beat-to-beat blood pressure (B3P). It can be used to monitor the effect of prolonged exposures to reduced gravitational environments and the effectiveness of various countermeasures.

A number of researchers have used pulse wave velocity (PWV) of blood in the arteries to infer the beat-to-beat blood pressure. There has been documentation of relative success, but a device that is able to provide the required accuracy and repeatability has not yet been developed. It has been demonstrated that an accurate and repeatable blood pressure measurement can be obtained by measuring the phase change (e.g., phase velocity), amplitude change, and distortion of the PPG waveforms along the brachial artery. The approach is based on comparing the full PPG

waveform between two points along the artery rather than measuring the time-of-flight. Minimizing the measurement separation and confining the measurement area to a single, well-defined artery allows the waveform to retain the general shape between the two measurement points. This allows signal processing of waveforms to determine the phase and amplitude changes.

Photoplethysmography, which measures changes in arterial blood volume, is commonly used to obtain heart rate and blood oxygen saturation. The digitized PPG signals are used as inputs into the beat-to-beat blood pressure measurement algorithm. The algorithm consists of the following main components:

- First harmonic isolation bandpass filters take the raw PPG signals and separate out the first harmonics.
- Three harmonic lowpass filters take the PPG signal and filter out all spectral components outside the first three harmonics. The first three harmonics are used for regeneration of the pulse pressure waveforms.
- Phase analysis engine takes the first harmonics of the PPG signals and computes the phase difference between them in real time using a cross-correlation-based algorithm. The phase difference is to the first order correlated to the MAP (mean arterial pressure).
- Compliance estimation engine takes information on the general shape of the waveforms and the phase delay to compute the local compliance of the

artery. The higher the arterial pressure, the higher the Young's modulus and thus the lower the compliance.

- MAP computation engine obtains the phase delay and compliance information and provides the mean arterial pressure.
- Waveform analysis engine takes the PPG signal containing the first three harmonics and provides the signal processing needed for compliance (elasticity) estimation and pulse pressure computation.
- Pulse pressure computation engine takes the filtered PPG signal and an estimate of the arterial compliance to regenerate the pulse waveform.
- B3P computation engine takes the MAP and the pulse pressure computations and combines them with a blood pressure model and calibration data to produce the final signal of interest — the beat-to-beat blood pressure.

This work was done by Yong Jin Lee of Linea Research Corporation for Johnson Space Center. Further information is contained in a TSP (see page 1).

In accordance with Public Law 96-517, the contractor has elected to retain title to this invention. Inquiries concerning rights for its commercial use should be addressed to:

*Linea Research Corporation
1020 Corporation Way
Suite 216
Palo Alto, CA 94303*

Refer to MSC-24601-1, volume and number of this NASA Tech Briefs issue, and the page number.

Measurement Techniques for Clock Jitter

New approach offers more advanced coded modulation techniques.

Lyndon B. Johnson Space Center, Houston, Texas

NASA is in the process of modernizing its communications infrastructure to accompany the development of a Crew Exploration Vehicle (CEV) to replace the shuttle. With this effort comes the oppor-

tunity to infuse more advanced coded modulation techniques, including low-density parity-check (LDPC) codes that offer greater coding gains than the current capability. However, in order to take

full advantage of these codes, the ground segment receiver synchronization loops must be able to operate at a lower signal-to-noise ratio (SNR) than supported by equipment currently in use.

At low SNR, the receiver symbol synchronization loop will be increasingly sensitive to transmitter timing jitter. Excessive timing jitter can cause bit slips in the receiver synchronization loop, which will in turn cause frame losses and potentially lead to receiver and/or decoder loss-of-lock. Therefore, it is necessary to investigate what symbol timing jitter requirements on the satellite transmitter are needed to support the next generation of NASA coded modulation techniques.

Measurements of ground segment receiver sensitivity to transmitter bit jitter were conducted using a satellite transponder and two different commercial staggered quadrature phase-shift keying (SQPSK) receivers. The symbol synchronizer loop transfer functions were characterized for each receiver. Symbol timing jitter was introduced at

the transmitter. Effects of sinusoidal (tone) jitter on symbol error rate (SER) degradation and symbol slip probability were measured. These measurements were used to define regions of sensitivity to phase, frequency, and cycle-to-cycle jitter characterizations. An assortment of other band-limited jitter waveforms was then applied within each region to identify peak or root-mean-square measures as a basis for comparability.

Receiver clock recovery loops that operate in low SNR ratio environments require that transmit clock jitter be constrained by several measures on different dimensions and operating regions. In this work, effects of transmit phase jitter (PhJ), frequency jitter (FJ), and cycle-to-cycle jitter (CCJ) were studied for sinusoidal and multi-tone jitter profiles on receiver performance. It was demonstrated that the receiver must have a loop band-

width tight enough to avoid cycle slips, but loose enough to track some movement in the data signal. Movement that a tight loop cannot track is usually manifested first as intersymbol interference (ISI) (SER degradation) and then ultimately as cycle slipping in the receiver.

Results from the tests indicate that the receiver symbol synchronization loop is more sensitive to certain types of symbol jitter and jitter frequencies, depending on the selection of the loop filter and damping ratio. A framework is provided to properly compose a transmit jitter mask depending on receiver design parameters such as damping ratio in order to limit receiver performance degradation at low SNR regions.

This work was done by Chatwin Lansdowne and Adam Schlesinger of Johnson Space Center. Further information is contained in a TSP (see page 1). MSC-24810-1

Lightweight, Miniature Inertial Measurement System

Goddard Space Flight Center, Greenbelt, Maryland

A miniature, lighter-weight, and highly accurate inertial navigation system (INS) is coupled with GPS receivers to provide stable and highly accurate positioning, attitude, and inertial measurements while being subjected to highly dynamic maneuvers. In contrast to conventional methods that use extensive, ground-based, real-time tracking and control units that are expensive, large, and require excessive amounts of power to operate, this method focuses on the development of an estimator that makes use of a low-cost, miniature accelerometer array fused with traditional measurement systems and GPS. Through the use of a posi-

tion tracking estimation algorithm, onboard accelerometers are numerically integrated and transformed using attitude information to obtain an estimate of position in the inertial frame. Position and velocity estimates are subject to drift due to accelerometer sensor bias and high vibration over time, and so require the integration with GPS information using a Kalman filter to provide highly accurate and reliable inertial tracking estimations.

The method implemented here uses the local gravitational field vector. Upon determining the location of the local gravitational field vector relative to two consecutive sensors, the orientation of

the device may then be estimated, and the attitude determined. Improved attitude estimates further enhance the inertial position estimates. The device can be powered either by batteries, or by the power source onboard its target platforms. A DB9 port provides the I/O to external systems, and the device is designed to be mounted in a waterproof case for all-weather conditions.

This work was done by Liang Tang of Impact Technologies and Agamemnon Crassidis of the Rochester Institute of Technology for Goddard Space Flight Center. Further information is contained in a TSP (see page 1). GSC-16132-1

Optical Density Analysis of X-Rays Utilizing Calibration Tooling to Estimate Thickness of Parts

This method uses off-the-shelf data analysis software and a digitized x-ray for nondestructive testing.

John F. Kennedy Space Center, Florida

This process is designed to estimate the thickness change of a material through data analysis of a digitized version of an x-ray (or a digital x-ray) containing the material (with the thickness in question) and various tooling. Using this process, it is possible to estimate a

material's thickness change in a region of the material or part that is thinner than the rest of the reference thickness. However, that same principle process can be used to determine the thickness change of material using a thinner region to determine thickening, or it can

be used to develop contour plots of an entire part.

Proper tooling must be used. An x-ray film with an S-shaped characteristic curve or a digital x-ray device with a product resulting in like characteristics is necessary. If a film exists with linear

characteristics, this type of film would be ideal; however, at the time of this reporting, no such film has been known. Machined components (with known fractional thicknesses) of a like material (similar density) to that of the material to be measured are necessary.

The machined components should have machined through-holes. For ease of use and better accuracy, the through-holes should be a size larger than 0.125 in. (≈ 3 mm). Standard components for this use are known as penetrameters or image quality indicators. Also needed is standard x-ray equipment, if film is used in place of digital equipment, or x-ray digitization equipment with proven conversion properties. Typical x-ray digitiza-

tion equipment is commonly used in the medical industry, and creates digital images of x-rays in DICOM format. It is recommended to scan the image in a 16-bit format. However, 12-bit and 8-bit resolutions are acceptable. Finally, x-ray analysis software that allows accurate digital image density calculations, such as Image-J freeware, is needed.

The actual procedure requires the test article to be placed on the raw x-ray, ensuring the region of interest is aligned for perpendicular x-ray exposure capture. One or multiple machined components of like material/density with known thicknesses are placed atop the part (preferably in a region of nominal and non-varying thick-

ness) such that exposure of the combined part and machined component lay-up is captured on the x-ray. Depending on the accuracy required, the machined component's thickness must be carefully chosen. Similarly, depending on the accuracy required, the lay-up must be exposed such that the regions of the x-ray to be analyzed have a density range between 1 and 4.5. After the exposure, the image is digitized, and the digital image can then be analyzed using the image analysis software.

This work was done by David Grau of Kennedy Space Center. Further information is contained in a TSP (see page 1). KSC-13206

Fuel Cell/Electrochemical Cell Voltage Monitor

Lyndon B. Johnson Space Center, Houston, Texas

A concept has been developed for a new fuel cell individual-cell-voltage monitor that can be directly connected to a multi-cell fuel cell stack for direct sub-stack power provisioning. It can also provide voltage isolation for applications in high-voltage fuel cell stacks. The technology consists of basic modules, each with an 8- to 16-cell input electrical measurement connection port. For each basic module, a power input connection would be provided for direct connection to a sub-stack of fuel cells in series within the larger stack. This power connection would allow for module power to be available in the range of 9-15 volts DC.

The relatively low voltage differences that the module would encounter from the input electrical measurement connection port, coupled with the fact that the module's operating power is supplied by the same substack voltage input (and so will be at similar voltage), provides for elimination of high-common-mode voltage issues within each module. Within each module, there would be options for analog-to-digital conversion and data transfer schemes.

Each module would also include a data-output/communication port. Each of these ports would be required to be either non-electrical (e.g., optically iso-

lated) or electrically isolated. This is necessary to account for the fact that the plurality of modules attached to the stack will normally be at a range of voltages approaching the full range of the fuel cell stack operating voltages. A communications/data bus could interface with the several basic modules. Options have been identified for command inputs from the spacecraft vehicle controller, and for output-status/data feeds to the vehicle.

This work was done by Arturo Vasquez of Johnson Space Center. For further information, contact the JSC Innovation Partnerships Office at (281) 483-3809. MSC-24592-1

Anomaly Detection Techniques With Real Test Data From a Spinning Turbine Engine-Like Rotor

These techniques are suitable for engine manufacturers and industries in aerospace and aviation.

John H. Glenn Research Center, Cleveland, Ohio

Online detection techniques to monitor the health of rotating engine components are becoming increasingly attractive to aircraft engine manufacturers in order to increase safety of operation and lower maintenance costs. Health monitoring remains a challenge to easily implement, especially in the presence of scattered loading conditions, crack size, component

geometry, and materials properties. The current trend, however, is to utilize non-invasive types of health monitoring or nondestructive techniques to detect hidden flaws and mini-cracks before any catastrophic event occurs. These techniques go further to evaluate material discontinuities and other anomalies that have grown to the level of critical defects that can lead to failure. Gener-

ally, health monitoring is highly dependent on sensor systems capable of performing in various engine environmental conditions and able to transmit a signal upon a predetermined crack length, while acting in a neutral form upon the overall performance of the engine system.

Spin simulation tests were conducted on a turbine engine-like rotor with and

without an artificially induced notch at different rotational loading speed levels. Health monitoring verification was performed by integrating three different advanced machine-learning algorithms for anomaly detection in continuous data streams from spinning tests of a subscale turbine engine-like rotor disk up to a speed of 10,000 rpm.

This study compares an outlier detection algorithm (Orca), one-class support vector machines (OCSVM), and the Inductive Monitoring System (IMS) for anomaly detection on the data streams. These techniques were used to inspect the experimental data under the same operating conditions employed in the tests, and using the measured vibration response (blade tip clearance) as a key input to check the viability of these techniques on detecting the disk anomalies and to evaluate the performance of each methodology. The performance of the algorithm is measured with respect to the detection

horizon for situations where fault information is available. Further, this work presents a select evaluation of an online health monitoring scheme of a rotating disk using a combination of high-caliber sensor technology, high-precision in-house spin test system facilities, and unprecedented data-driven fault detection methodologies.

The methodologies applied in this study can be considered as a model-based reasoning approach to engine health monitoring. Typical model-based reasoning techniques compare a system model or simulation with system sensor data to detect deviations between values predicted by the model and those produced by the actual system. In fact, a model-based reasoner uses the collected system parameter values as input to a simulation and determines if a particular set of input values is consistent with the simulation model. When the values are not consistent with the model, a “conflict” occurs, indicating that the sys-

tem operation is off nominal. The results obtained showed that the detection algorithms are capable of predicting anomalies in the rotor disk with very good accuracy. Each detection scheme performed differently under the same experimental conditions, and each delivered a different level of precision in terms of detecting a fault in the rotor. Overall rating showed that both the Orca and OCVSM performed better than the IMS technique.

This work was done by Ali Abdul-Aziz, Mark R. Woike, Nikunj C. Oza, and Bryan L. Matthews of Glenn Research Center. Further information is contained in a TSP (see page 1).

Inquiries concerning rights for the commercial use of this invention should be addressed to NASA Glenn Research Center, Innovative Partnerships Office, Attn: Steven Fedor, Mail Stop 4-8, 21000 Brookpark Road, Cleveland, Ohio 44135. Refer to LEW-18758-1.

Measuring Air Leaks Into the Vacuum Space of Large Liquid Hydrogen Tanks

John F. Kennedy Space Center, Florida

Large cryogenic liquid hydrogen tanks are composed of inner and outer shells. The outer shell is exposed to the ambient environment while the inner shell holds the liquid hydrogen. The region between these two shells is evacuated and typically filled with a powder-like insulation to minimize radiative coupling between the two shells. A technique was developed for detecting the presence of an air leak from the outside environment into this evacuated region.

These tanks are roughly 70 ft (≈ 21 m) in diameter (outer shell) and the inner shell is roughly 62 ft (≈ 19 m) in diameter, so the evacuated region is about 4 ft (≈ 1 m) wide.

A small leak’s primary effect is to increase the boil-off of the tank. It was preferable to install a more accurate fill level sensor than to implement a boil-off meter. The fill level sensor would be composed of an accurate pair of pressure transducers that would essentially

weigh the remaining liquid hydrogen. This upgrade, allowing boil-off data to be obtained weekly instead of over several months, is ongoing, and will then provide a relatively rapid indication of the presence of a leak.

This work was done by Robert Youngquist, Stanley Starr, and Mark Nurge of Kennedy Space Center. Further information is contained in a TSP (see page 1). KSC-13211

Antenna Calibration and Measurement Equipment

NASA’s Jet Propulsion Laboratory, Pasadena, California

A document describes the Antenna Calibration & Measurement Equipment (ACME) system that will provide the Deep Space Network (DSN) with instrumentation enabling a trained RF engineer at each complex to perform antenna calibration measurements and to generate antenna calibration data. This data includes continuous-scan auto-bore-based data acquisition with all-sky data gathering in support of 4th order

pointing model generation requirements. Other data includes antenna subreflector focus, system noise temperature and tipping curves, antenna efficiency, reports system linearity, and instrument calibration.

The ACME system design is based on the on-the-fly (OTF) mapping technique and architecture. ACME has contributed to the improved RF performance of the DSN by approximately a

factor of two. It improved the pointing performances of the DSN antennas and productivity of its personnel and calibration engineers.

This work was done by David J. Rochblatt and Manuel Vazquez Cortes of Caltech for NASA’s Jet Propulsion Laboratory. Further information is contained in a TSP (see page 1). NPO-47599



■ Glass Solder Approach for Robust, Low-Loss, Fiber-to-Waveguide Coupling

Goddard Space Flight Center, Greenbelt, Maryland

The key advantages of this approach include the fact that the index of interface glass (such as Pb glass $n = 1.66$) greatly reduces Fresnel losses at the fiber-to-waveguide interface, resulting in lower optical losses. A contiguous structure cannot be misaligned and readily lends itself for use on aircraft or space operation. The epoxy-free, fiber-to-waveguide interface provides an optically pure, sealed interface for low-loss, high-power coupling. Proof of concept of this approach has included successful attachment of the low-melting-temperature

glass to the x - y plane of the crystal, successful attachment of the low-melting-temperature glass to the end face of a standard SMF (single-mode fiber), and successful attachment of a wetted low-melting-temperature glass SMF to the end face of a KTP crystal.

There are many photonic components on the market whose performance and robustness could benefit from this coupling approach once fully developed. It can be used in a variety of fiber-coupled waveguide-based components, such as frequency conversion modules,

and amplitude and phase modulators. A robust, epoxy-free, contiguous optical interface lends itself to components that require low-loss, high-optical-power handling capability, and good performance in adverse environments such as flight or space operation.

This work was done by Shirley McNeil, Philip Battle, and Todd Hawthorne of AdvR, Inc.; and John Lower, Robert Wiley, and Brett Clark of 3SAE Technologies, Inc. for Goddard Space Flight Center. Further information is contained in a TSP (see page 1). GSC-16348-1

■ Lightweight Metal Matrix Composite Segmented for Manufacturing High-Precision Mirrors

New approach is examined to reduce production costs.

Goddard Space Flight Center, Greenbelt, Maryland

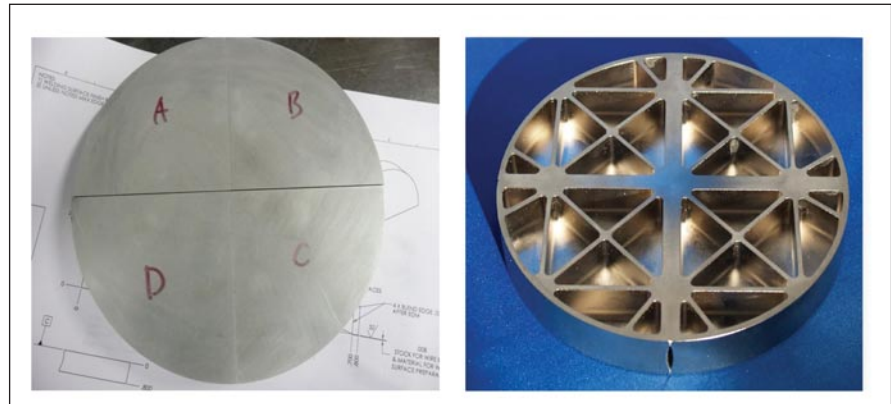
High-precision mirrors for space applications are traditionally manufactured from one piece of material, such as lightweight glass “sandwich” or beryllium. The purpose of this project was to develop and test the feasibility of a manufacturing process capable of producing mirrors out of welded segments of AlBeMet[®] (AM162H). AlBeMet[®] is a HIP’d (hot isostatic pressed) material containing approximately 62% beryllium and 38% aluminum. As a result, AlBeMet[®] shares many of the benefits of both of those materials for use in high performance mirrors, while minimizing many of their weaknesses.

AlBeMet[®] machines more like aluminum than beryllium, but retains many of the beneficial structural characteristics of beryllium, such as a lower coefficient of thermal expansion (CTE), greater stiffness, and lower density than aluminum. AlBeMet[®] also has as a key characteristic that it can be electron-beam welded, and AlBeMet[®] has been demonstrated as a suitable material for use as an optical substrate. These last

two characteristics were central to the selection of AlBeMet[®] as the material to be used in the construction of the segmented mirror. In order to effectively compare the performance of the monolithic and the segmented mirror, a plano mirror was designed.

A plano mirror is the best design, as it minimizes the effect of extraneous factors on the performance of the final mirror, such as the skill of the polisher to

achieve the proper prescription. A plano mirror will also theoretically retain the same prescription when segmented and then reassembled. Any material lost to the kerf will not change the prescription, unlike, for example, a spherical mirror whose radius of curvature will become smaller with the loss of material. The mirror design also incorporates light-weighting cavities and stiffening ribs, as is typical in space-based mirror



Front of the welded mirror substrate. Back of the finished mirror.

design. Thicker ribs were required along the proposed cutting/welding lines to facilitate the machining of those surfaces when the mirror was segmented. The mirror was designed to be cut into four (4) equal segments. As a result, the thicker ribs ran perpendicular to each other through the center of the mirror.

The monolithic mirror was machined and ground by closely following Materion's suggested fabrication process for AlBeMet[®], including stabilization, temperature cycling, and in-process inspection checks. Once the flatness had been obtained, the mirror was sent for nickel plating. The mirror was plated with high-phosphorous nickel to a thickness between 0.003 and 0.004 in. (≈ 0.076 and 0.102 mm) in accordance with specification AMS 2404, class I. After nickel-plating, the mirror was stabilized and then polished to obtain a finished optic. In the end, the monolithic mirror achieved a surface figure of nearly $\frac{1}{4} \lambda$ (0.286λ) at 633 nm with a surface roughness of 15 \AA rms.

The monolithic mirror was then prepared to be segmented and welded. The nickel-plating on the mirror had to be completely stripped off in order to facilitate welding. The mirror was cut into four quarters using a wire EDM process. The segments were stabilized and cleaned before being delivered to Materion for the welding process. The welds along the mirror surface were done first and the mirror flipped and aligned, and the backside, along the bottom of the ribs, was welded.

Following welding, one first had to remove enough material from the mirror surface to get below any surface damage or other irregularities caused by the weld. A small amount of material was also removed from the backside of the mirror, simply to clean up the appearance of that weld. The mirror was stress relieved before being ground to the proper flatness requirement, after which the mirror was inspected and sent out for nickel plating.

The returned mirror underwent the grinding and polishing process in the same manner as that used on the monolithic mirror. The mirror was ground and polished until it achieved a surface figure of less than 1 (at 633 nm), temperature cycled for stabilization, and then re-measured. In the end, the segmented mirror achieved a surface figure of less than 0.7 at 633 nm with a surface roughness measured at 16.5 \AA . It is very probable that a better surface figure could have been achieved on the segmented mirror, but budget constraints of this Phase I project prevented further efforts.

Based on the results presented, the feasibility of creating high-performance mirrors out of welded segments of AlBeMet[®] has been proven and has the potential for being used in a full-size astronomical mirror.

This work was done by Vladimir Vudler of Hardric Laboratories, Inc. for Goddard Space Flight Center. Further information is contained in a TSP (see page 1). GSC-16165-1

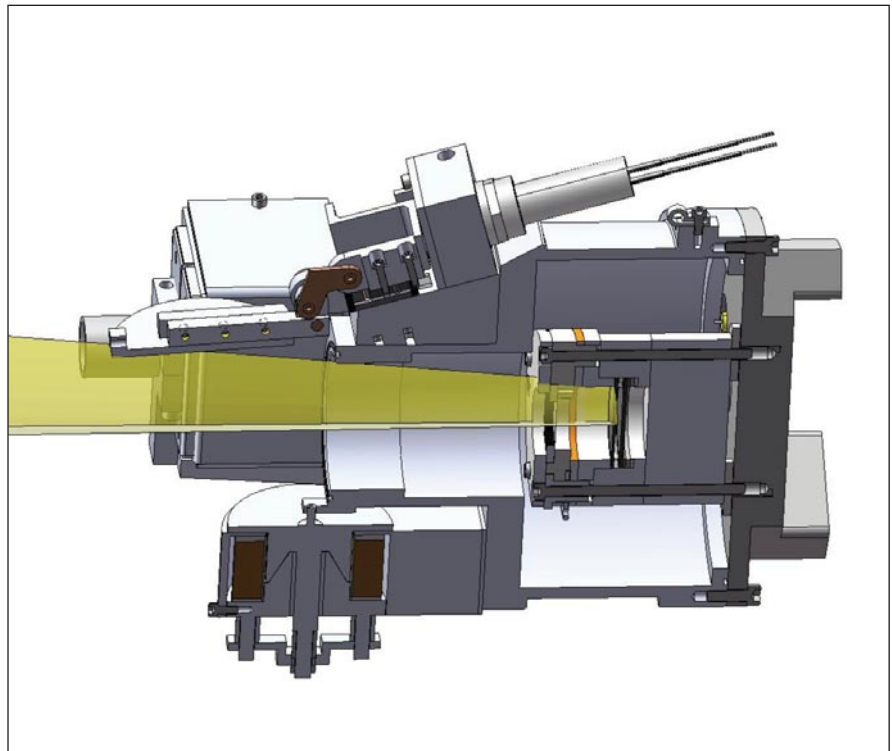
Plasma Treatment To Remove Carbon From Indium UV Filters

Hydrogen plasma cleaning is used in sterilization applications in healthcare as an alternative to autoclaving.

NASA's Jet Propulsion Laboratory, Pasadena, California

The sounding rocket experiment FIRE (Far-ultraviolet Imaging Rocket Experiment) will improve the science community's ability to image a spectral region hitherto unexplored astronomically. The imaging band of FIRE (≈ 900 to $1,100 \text{ \AA}$) will help fill the current wavelength imaging observation hole existing from $\approx 620 \text{ \AA}$ to the GALEX band near $1,350 \text{ \AA}$. FIRE is a single-optic prime focus telescope with a 1.75-m focal length. The bandpass of 900 to 1100 \AA is set by a combination of the mirror coating, the indium filter in front of the detector, and the salt coating on the front of the detector's microchannel plates. Critical to this is the indium filter that must reduce the flux from Lyman-alpha at $1,216 \text{ \AA}$ by a minimum factor of 10^{-4} . The cost of this Lyman-alpha removal is that the filter is not fully transparent at the desired wavelengths of 900 to $1,100 \text{ \AA}$.

Recently, in a project to improve the performance of optical and solar blind detectors, JPL developed a plasma process capable of removing carbon contamination from indium metal. In this work, a low-power, low-temperature



A cutaway view shows the **Detector Assembly and Filter**. The indium filter sits just in front of the detector plates in the light beam (yellow cone) at the orange ring.

hydrogen plasma reacts with the carbon contaminants in the indium to form methane, but leaves the indium metal surface undisturbed. This process was recently tested in a proof-of-concept experiment with a filter provided by the University of Colorado. This initial test on a test filter showed improvement in transmission from 7 to 9 percent near 900 Å with no process optimization applied. Further improvements in this performance were readily achieved to bring the total transmission to 12% with optimization to JPL's existing process.

A low-power, hydrogen plasma treatment is generated in a PlasmaTherm RIE etcher using a mixture of argon and hy-

drogen gas. The gas ratio is optimized in order to control the following variables: bias voltage, atomic hydrogen content, and substrate temperature. Low bias voltage is required to avoid mechanically degrading the filters by sputtering the indium foil. High atomic hydrogen content is required to enhance the carbon removal rate. Low substrate temperature is required to avoid deformation of the indium foil due to sagging. Those variables are optimized around MFC (mass flow controller) setpoints of 25 sccm argon and 7 sccm hydrogen.

This work was done by Harold F. Greer and Shouleh Nikzad of Caltech, and Matthew Beasley and Brennan Gantner of the Univer-

sity of Colorado for NASA's Jet Propulsion Laboratory. Further information is contained in a TSP (see page 1).

In accordance with Public Law 96-517, the contractor has elected to retain title to this invention. Inquiries concerning rights for its commercial use should be addressed to:

*Innovative Technology Assets Management
JPL*

Mail Stop 202-233

4800 Oak Grove Drive

Pasadena, CA 91109-8099

E-mail: iaoffice@jpl.nasa.gov

Refer to NPO-47400, volume and number of this NASA Tech Briefs issue, and the page number.



Telerobotics Workstation (TRWS) for Deep Space Habitats

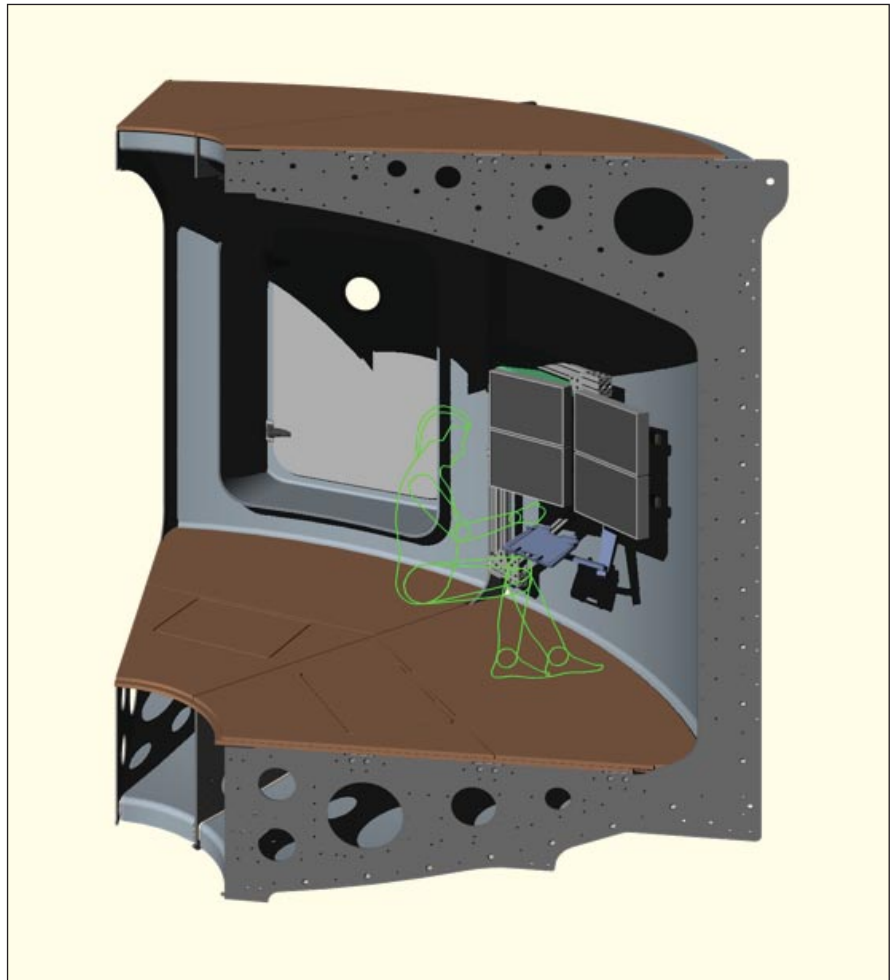
This multi-display computer workstation can be adjusted for a variety of configurations.

NASA's Jet Propulsion Laboratory, Pasadena, California

On medium- to long-duration human spaceflight missions, latency in communications from Earth could reduce efficiency or hinder local operations, control, and monitoring of the various mission vehicles and other elements. Regardless of the degree of autonomy of any one particular element, a means of monitoring and controlling the elements in real time based on mission needs would increase efficiency and response times for their operation. Since human crews would be present locally, a local means for monitoring and controlling all the various mission elements is needed, particularly for robotic elements where response to interesting scientific features in the environment might need near-instantaneous manipulation and control.

One of the elements proposed for medium- and long-duration human spaceflight missions, the Deep Space Habitat (DSH), is intended to be used as a remote residence and working volume for human crews. The proposed solution for local monitoring and control would be to provide a workstation within the DSH where local crews can operate local vehicles and robotic elements with little to no latency.

The Telerobotics Workstation (TRWS) is a multi-display computer workstation mounted in a dedicated location within the DSH that can be adjusted for a variety of configurations as required. From an Intra-Vehicular Activity (IVA) location, the TRWS uses the Robot Application Programming Interface Delegate (RAPID) control environment through the local network to remotely monitor and control vehicles and robotic assets located outside the pressurized volume in the immediate vicinity or at low-latency distances from the habitat. The multiple display area of the TRWS allows the crew to have numerous windows open with live video feeds, control windows, and data browsers, as well as local monitoring and control of the DSH and associated systems.



The Telerobotics Workstation (TRWS) swing frame enables the mounted computer workstation to be adjusted for a variety of configurations.

The novelty of the TRWS comes from the integration and configuration of various software and hardware elements within the context of the DSH environment. Controls, communications, power status, situational awareness information, and telemetry — though employing conventional and sometimes commercial off-the-shelf (COTS) equipment — are displayed in a unique operational environment that must compete with crew attention in a fully functional habitat. The TRWS RAPID software, hardware, structural configuration, ergo-

nomics, and human factors combine to provide the crew with an efficient tool for carrying out mission remote asset control objectives.

This work was done by David S. Mittman, Alan S. Howe, and Recaredo J. Torres of Caltech; Jennifer L. Rochlis Zumbado and Kimberly A. Hambuchen of Johnson Space Center; and Matthew Demel and Christopher C. Chapman of JSC Jacobs Technology for NASA's Jet Propulsion Laboratory. Further information is contained in a TSP (see page 1). NPO-48503

Single-Pole Double-Throw MMIC Switches for a Microwave Radiometer

Switches reduce the effect of gain and noise instabilities.

NASA's Jet Propulsion Laboratory, Pasadena, California

In order to reduce the effect of gain and noise instabilities in the RF chain of a microwave radiometer, a Dicke radiometer topology is often used, as in the case of the proposed surface water and ocean topography (SWOT) radiometer instrument. For this topology, a single-pole double-throw (SPDT) microwave switch is needed, which must have low insertion loss at the radiometer channel frequencies to minimize the overall receiver noise figure. Total power radiometers are limited in accuracy due to the continuous variation in gain of the receiver. Currently, there are no switches in the market that can provide these characteristics at 92, 130, and 166 GHz as needed for the proposed SWOT radiometer instrument.

High-frequency SPDT switches were developed in the form of monolithic mi-

crowave integrated circuits (MMICs) using 75- μm indium phosphide (InP) PIN-diode technology. These switches can be easily integrated into Dicke switched radiometers that utilize microstrip technology. The MMIC switches operate from 80 to 105 GHz, 90 to 135 GHz, and 160 to 185 GHz. The 80- to 105-GHz switches have been tested and have achieved <2-dB insertion loss, >15-dB return loss (>18 dB for the asymmetric design), and >15-dB isolation. The isolation can be tuned to achieve >20-dB isolation from 85 to 103 GHz. The 90- to 135-GHz SPDT switch has achieved <2-dB insertion loss, >15-dB return loss, and 8- to 12-dB isolation. However, it has been shown that the isolation of this switch can also be improved. Although the 160- to 185-GHz switch has been fabricated, it has not yet been measured at

the time of this reporting. Simulation results predict this switch will have <2-dB insertion loss, >20-dB return loss, and >20-dB isolation.

The switches can be used for a radiometer such as the one proposed for the SWOT Satellite Mission whose three channels at 92, 130, and 166 GHz would allow for wet-tropospheric path delay correction near coastal zones and over land. This feat is not possible with the current Jason-class radiometers due to their lower frequency signal measurement and thus lower resolution.

The design work was done by Oliver Montes, Douglas E. Dawson, and Pekka P. Kangaslahti of Caltech for NASA's Jet Propulsion Laboratory. The processing of the InP MMIC circuits was done by Kwok Loi and Augusto Gutierrez from NGST. Further information is contained in a TSP (see page 1), NPO-48083

On Shaft Data Acquisition System (OSDAS)

Applications include helicopter rotor testing, onboard liquid/solid rocket engine data acquisition, and gas-turbine-engine health monitoring.

Marshall Space Flight Center, Alabama

On Shaft Data Acquisition System (OSDAS) is a rugged, compact, multiple-channel data acquisition computer system that is designed to record data from instrumentation while operating under extreme rotational centrifugal or gravitational acceleration forces. This system, which was developed for the Heritage Fuel Air Turbine Test (HFATT) program, addresses the problem of recording multiple channels of high-sample-rate data on most any rotating test article by mounting the entire acquisition computer onboard with the turbine test article. With the limited availability of slip ring wires for power and communication, OSDAS utilizes its own resources to provide independent power and amplification for each instrument. Since OSDAS utilizes standard PC technology as well as shared code interfaces with the next-generation, real-time health monitoring system (SPARTAA — Scalable Parallel Architecture for Real Time Analysis and Acquisition), this system could be expanded beyond its current capabilities, such as

providing advanced health monitoring capabilities for the test article.

High-conductor-count slip rings are expensive to purchase and maintain, yet only provide a limited number of conductors for routing instrumentation off the article and to a stationary data acquisition system. In addition to being limited to a small number of instruments, slip rings are prone to wear quickly, and introduce noise and other undesirable characteristics to the signal data. This led to the development of a system capable of recording high-density instrumentation, at high sample rates, on the test article itself, all while under extreme rotational stress.

OSDAS is a fully functional PC-based system with 48 channels of 24-bit, high-sample-rate input channels, phase synchronized, with an onboard storage capacity of over 1/2-terabyte of solid-state storage. This recording system takes a novel approach to the problem of recording multiple channels of instrumentation, integrated with the test article itself, pack-

aged in a compact/rugged form factor, consuming limited power, all while rotating at high turbine speeds.

The hardware components were oriented, secured, and encapsulated by a variety of novel application techniques that allow for the system to continue operation under rotational stress. This full, custom-hardened system was designed to be a comprehensive solution to attaching directly to instrumentation (without external sensor power supplies and amplification). Instead, all instrumentation has a dedicated power supply, integrated inside OSDAS, with the ability to withstand electrical faults (short circuits, etc.) without compromising other sensors. The amplification required for each sensor was configurable at build time to match that of the Kulite instrumentation used in the HFATT article. The entire computing, storage, and acquisition hardware system was custom-encapsulated in a thermally conductive medium that allows heat to passively dissipate by air via the outer shell (indoor/out-

door environmental conditions) or by conduction cooling in space conditions.

OSDAS is a comprehensive, high-capacity acquisition system capable of withstanding extreme rotational forces. The existing products on the market are either limited in channel capacity, bandwidth, or simply not capable of withstanding physical stress. As part of the build process, a variety of mounting and encapsulation techniques was utilized, which ensures the system can withstand harsh rotational stresses. OSDAS employs the use of standard PC technology. The system was built to share a code interface with that of the SPARTAA, other-

wise known as the next-generation, real-time vibration monitoring system (RTVMS). This allows OSDAS to be expanded in the future to incorporate real-time health monitoring of the test article hardware.

OSDAS employs a common hardware-mounting interface that allows the acquisition system to be adapted to a variety of test articles and environments. With the use of built-in sensor amplification and independent power supplies, a total sensor acquisition solution was provided. While acquisition storage capacity and channel counts were limited initially by the desire of a small/compact form factor, further

expansion beyond 48 channels and multi-terabyte solutions is possible. For the final system checkout, OSDAS was subjected to speeds over 15,000 RPM (maximum facility capability). A continuous Ethernet connection was maintained throughout the checkout and test series.

This work was done by Marc Pedings, Shawn DeHart, Jason Formby, and Charles Naumann of Optical Sciences Corporation for Marshall Space Flight Center. For more information, contact Sammy Nabors, MSFC Commercialization Assistance Lead, at sammy.a.nabors@nasa.gov. Refer to MFS-32908-1.

ASIC Readout Circuit Architecture for Large Geiger Photodiode Arrays

Commercial applications include 3D imaging, positron emission tomography (PET), laser ranging (LADAR), night vision, and surveillance.

Goddard Space Flight Center, Greenbelt, Maryland

The objective of this work was to develop a new class of readout integrated circuit (ROIC) arrays to be operated with Geiger avalanche photodiode (GPD) arrays, by integrating multiple functions at the pixel level (smart-pixel or active pixel technology) in 250-nm CMOS (complementary metal oxide semiconductor) processes. In order to pack a maximum of functions within a minimum pixel size, the ROIC array is a full, custom application-specific integrated circuit (ASIC) design using a mixed-signal CMOS process with compact primitive layout cells.

The ROIC array was processed to allow assembly in bump-bonding technology with photon-counting infrared detector arrays into 3-D imaging cameras (LADAR). The ROIC architecture was designed to work with either common-anode Si GPD arrays or common-cathode InGaAs GPD arrays. The current ROIC pixel design is hardwired prior to processing one of the two GPD array configurations, and it has the provision to allow soft reconfiguration to either array (to be implemented into the next ROIC array generation). The ROIC pixel architecture implements the Geiger avalanche quenching, bias, reset, and time to digital conversion (TDC) functions in full-digital design, and uses time domain over-sampling (vernier) to allow high temporal resolution at low clock rates, increased data

yield, and improved utilization of the laser beam.

The non-uniformity of the breakdown voltage over large GPD arrays (a serious concern in InGaAs GPD arrays) is partially corrected by a digital-to-analog circuit, capable of detecting the first breakdown event at pixel level, storing the breakdown voltage bin, and correcting for the breakdown voltage excursion. The correction is written at the pixel level. It is performed once at the first power-up and could be repeated any time prior to field operation after ROIC hard reset. Implementing this feature is critical for large and very large GPD arrays, for which I/O limitations impose on-die time binning on multiple pixels.

A pixel-level interface integrated into the ROIC pixel was developed to work with the GPD pixel (active quenching or AQC). The AQC interface detects the Geiger pulse, quenches the Geiger avalanche, and then resets (drains) the charge at the GPD-AQC node. The ROIC-GPD array is fully gated — GATE enable generates the START signal for the pixel-level TDCs and biases the GPD pixel above the breakdown voltage. The stop event in TDC is driven by the AQC output (following the photon detection registration) and identifies the time stamp with respect to the system clock generating the synchronized GATE (START) signal. The signal is fed

through multiple taps for fine time sampling (vernier bits) to a synchronized random counter. A programmable delay in the time vernier module allows extending the dynamic range without adding counter bits to the raw range TDC module, but at the expense of decreased timing resolution. ROIC arrays processed in 250-nm CMOS allowed increasing the count rate of the Geiger arrays (less than 20-ns reset) and reading out the time stamp of Geiger events detected in each pixel with 350-ps timing resolution. Fine time sampling is created by using redundant clock phase shifting as a time vernier, thus allowing the pixel to over-sample the time domain at low clock frequency (200 MHz), and thus decreasing the uncertainty due to setup time violations and improving the utilization of the laser pulses. The programmable delay allows also super-fine timing — in this mode the ROIC should be capable of 175-ps timing resolution. The row-column driver, integrated with the ROIC array, enables shifting sequentially the row data. The implementation into 16x32 or mosaic 32x32 pixel ROIC arrays should be scalable to much larger ROIC/GPD arrays.

This work was done by Stefan Vasile and Jerold Lipson of aPeak Inc. for Goddard Space Flight Center. Further information is contained in a TSP (see page 1). GSC-16107-1

Flexible Architecture for FPGAs in Embedded Systems

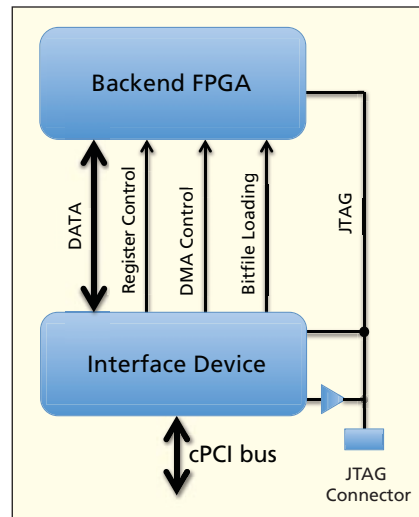
A small device simplifies FPGA development in cPCI systems.

NASA's Jet Propulsion Laboratory, Pasadena, California

Commonly, field-programmable gate arrays (FPGAs) being developed in cPCI embedded systems include the bus interface in the FPGA. This complicates the development because the interface is complicated and requires a lot of development time and FPGA resources. In addition, flight qualification requires a substantial amount of time be devoted to just this interface.

Another complication of putting the cPCI interface into the FPGA being developed is that configuration information loaded into the device by the cPCI microprocessor is lost when a new bit file is loaded, requiring cumbersome operations to return the system to an operational state.

Finally, SRAM-based FPGAs are typically programmed via specialized cables and software, with programming files being loaded either directly into the FPGA, or into PROM devices. This can be cumbersome when doing FPGA development in an embedded environment, and does not have an easy path to flight. Currently, FPGAs used in space applications are usually programmed via multiple space-qualified PROM devices that are physically large and require extra circuitry (typically including



The **cPCI Interface** is a common interface between the cPCI bus and the backend FPGA. It is implemented as a separate interface device on the cPCI bus.

a separate one-time programmable FPGA) to enable them to be used for this application.

This technology adds a cPCI interface device with a simple, flexible, high-performance backend interface supporting multiple backend FPGAs. It includes a mechanism for programming the FPGAs

directly via the microprocessor in the embedded system, eliminating specialized hardware, software, and PROM devices and their associated circuitry. It has a direct path to flight, and no extra hardware and minimal software are required to support reprogramming in flight. The device added is currently a small FPGA, but an advantage of this technology is that the design of the device does not change, regardless of the application in which it is being used. This means that it needs to be qualified for flight only once, and is suitable for one-time programmable devices or an application specific integrated circuit (ASIC). An application programming interface (API) further reduces the development time needed to use the interface device in a system.

This work was done by Duane I. Clark and Chester N. Lim of Caltech for NASA's Jet Propulsion Laboratory. Further information is contained in a TSP (see page 1).NPO-48424

The software used in this innovation is available for commercial licensing. Please contact Daniel Broderick of the California Institute of Technology at danielb@caltech.edu. Refer to NPO-48424.



❏ Polyurea-Based Aerogel Monoliths and Composites

These aerogels can be used in portable apparatus for warming, storing, and/or transporting food and medicine, and can be recycled for fillers for conventional plastics.

Lyndon B. Johnson Space Center, Houston, Texas

A flexible, organic polyurea-based aerogel insulation material was developed that will provide superior thermal insulation and inherent radiation protection for government and commercial applications. The rubbery polyurea-based aerogel exhibits little dustiness, good flexibility and toughness, and durability typical of the parent polyurea polymer, yet with the low density and superior insulation properties associated with aerogels. The thermal conductivity values of polyurea-based aerogels at lower temperature under vacuum pressures are very low and better than that of silica aerogels.

Flexible, rubbery polyurea-based aerogels are able to overcome the weak and brittle nature of conventional inorganic and organic aerogels, including polyisocyanurate aerogels, which are generally prepared with the one similar component to polyurethane rubber aerogels. Additionally, with higher content of hydrogen in their structures, the polyurea rubber-based aerogels will also provide inherently better radiation protection than those of inorganic and carbon aerogels. The aerogel materials also demonstrate good hydrophobicity due to their hydrocarbon molecular structure.

There are several strategies to overcoming the drawbacks associated with the weakness and brittleness of silica aerogels. Development of the flexible fiber-reinforced silica aerogel composite blanket has proven to be one promising approach, providing a conveniently fielded form factor that is relatively robust in industrial environments compared to silica aerogel monoliths. However, the flexible, silica aerogel composites still have a brittle, dusty character that may be undesirable, or even intolerable, in certain application environments. Although the cross-linked organic aerogels, such as resorcinol-formaldehyde (RF), polyisocyanurate, and cellulose aerogels, show very high impact strength, they are also very brittle with little elongation (i.e., less rubbery). Also, silica and carbon aerogels are less efficient radiation shielding materials due to their lower content of hydrogen element.

The invention involves mixing at least one isocyanate resin in solvent along with a specific amount of at least one polyamine hardener. The hardener is selected from a group of polyoxyalkyleneamines, amine-based polyols, or a mixture thereof. Mixing is performed in the presence of a catalyst and

reinforcing inorganic and/or organic materials, and the system is then subjected to gelation, aging, and supercritical drying. The aerogels will offer exceptional flexibility, excellent thermal and physical properties, and good hydrophobicity.

The rubbery polyurea-based aerogels are very flexible with no dust and hydrophobic organics that demonstrated the following ranges of typical properties: densities of 0.08 to 0.293 g/cm³, shrinkage factor (raerogel/rtarget) = 1.6 to 2.84, and thermal conductivity values of 15.2 to 20.3 mW/m K.

This work was done by Je Kyun Lee of Aspen Aerogels, Inc. for Johnson Space Center. Further information is contained in a TSP (see page 1).

In accordance with Public Law 96-517, the contractor has elected to retain title to this invention. Inquiries concerning rights for its commercial use should be addressed to:

*Aspen Aerogels, Inc.
30 Forbes Road, Building B
Northborough, MA 01532
Phone No.: (508) 691-1111
Fax No.: (508) 691-1200*

Refer to MSC-24214-1, volume and number of this NASA Tech Briefs issue, and the page number.

❏ Resin-Impregnated Carbon Ablator: A New Ablative Material for Hyperbolic Entry Speeds

From surface temperatures as high as ≈3,000 °C, the measured back temperature is only 50 °C.

Goddard Space Flight Center, Greenbelt, Maryland

Ablative materials are required to protect a space vehicle from the extreme temperatures encountered during the most demanding (hyperbolic) atmospheric entry velocities, either for probes launched toward other celestial bodies, or coming back to Earth from deep space missions. To that effect, the

resin-impregnated carbon ablator (RICA) is a high-temperature carbon/phenolic ablative thermal protection system (TPS) material designed to use modern and commercially viable components in its manufacture. Heritage carbon/phenolic ablators intended for this use rely on materials

that are no longer in production (i.e., Galileo, Pioneer Venus); hence the development of alternatives such as RICA is necessary for future NASA planetary entry and Earth re-entry missions. RICA's capabilities were initially measured in air for Earth re-entry applications, where it was exposed to a heat



Figure 1. RICA Sample during plasma wind tunnel testing.

flux of 14 MW/m² for 22 seconds. Methane tests were also carried out for potential application in Saturn's moon Titan, with a nominal heat flux of 1.4 MW/m² for up to 478 seconds. Three slightly different material formulations

RICA	Phenolic Content (~%)	Carbon Content (~%)	Density (gm/ml)	Plasma Wind Tunnel Heat Flux (MW/m ²)	Heat Duration (s)	Integrated Heat Input (J/m ²)	Mass Loss (gm)	Average Recession (mm)	Average Surface Temp from Pyrometer (c)	Average Thermal Gradient (K/mm)	Heat of Ablation (J/kg)
5C	17	83	1.41	1.4	478	6.69E+08	7.84	4.218	1978.1	44.37	49E.+07
5A(1)	27	73	1.39	14	22	3.08E+08	3.33	1.96	3336.1	34.32	1.1E+08
3A	24	76	1.36	1.4	478	6.69E+08	3.32	0.342	1962.5	54.50	8.5E+07
5B	33	67	1.37	1.4	476	6.67E+08	3.73	1.217	1990.8	53.68	7.7E+07
3B	31	69	1.35	1.4	477	6.67E+08	3.70	1.143	1967.5	51.11	8.5E+07

(1) Tested in Air; all others tested in Methane

Table. Material Properties and initial test results.

were manufactured and subsequently tested at the Plasma Wind Tunnel of the University of Stuttgart in Germany (PWK1) in the summer and fall of 2010. The TPS' integrity was well preserved in most cases, and results show great promise.

There are several major elements involved in the creation of a successful ablative TPS material: the choice of fabric and resin formulation is only the beginning. The actual processing involved in manufacturing involves a careful choice of temperature, pressure, and time. This manufacturing process must result in a material that survives heat loads with no de-lamination or spallation. Several techniques have been developed to achieve this robustness. Variants of RICA's material showed no delamination or spallation at intended heat flux levels, and their potential thermal protection capability was demonstrated. Three resin formulations were tested in two separate samples each manufactured under

slightly different conditions. A total of six samples were eventually chosen for test at the PWK1. Material performance properties and results for five of those are shown in the table. In the most extreme case, the temperature dropped from ≈3,000 to 50 °C across 1.8 cm, demonstrating the material's effectiveness in protecting a spacecraft's structure from the searing heat of entry.

With a manufacturing process that can be easily re-created, RICA has proven to be a viable choice for high-speed hyperbolic entry trajectories, both in methane (Titan) as well as in air (Earth) atmospheres. Further assessment and characterization of spallation and an exact determination of its onset heat flux (if present for intended applications) still remain to be measured.

This work was done by Jaime Esper of Goddard Space Flight Center and Michael Lengowski of the University of Stuttgart. Further information is contained in a TSP (see page 1). GSC-16183-1

Self-Cleaning Particulate Prefilter Media

This technology has application for air filter manufacturers for self-cleaning particulate prefilters.

John H. Glenn Research Center, Cleveland, Ohio

A long-term space mission requires efficient air revitalization performance to sustain the crew. Prefilter and particulate air filter media are susceptible to rapid fouling that adversely affects their performance and can lead to catastrophic failure of the air revitalization system, which may result in mission failure. For a long-term voyage, it is impractical to carry replacement particulate prefilter and filter modules due to the usual limitations in size, volume, and weight. The only solution to this problem is to reagentlessly regenerate

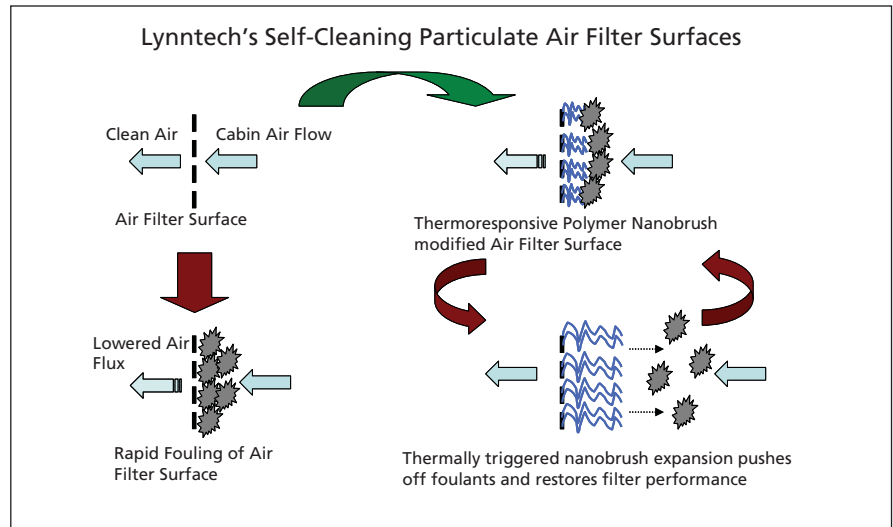
prefilter and filter media in place. A method was developed to modify the particulate prefilter media to allow them to regenerate reagentlessly, and in place, by the application of modest thermocycled transverse or reversed airflows. The innovation may allow NASA to close the breathing air loop more efficiently, thereby sustaining the vision for manned space exploration missions of the future.

A novel, self-cleaning coatings technology was developed for air filter media surfaces that allows reagentless in-place

regeneration of the surface. The technology grafts thermoresponsive and nonspecific adhesion minimizing polymer nanolayer brush coatings from the prefilter media. These polymer nanolayer brush architectures can be triggered to contract and expand to generate a "pushing-off" force by the simple application of modestly thermocycled (i.e. cycling from ambient cabin temperature to 40 °C) air streams. The nonspecific adhesion-minimizing properties of the coatings do not allow the particulate foulants to adhere strongly to the filter

media, and thermocycled air streams applied to the media allow easy detachment and in-place regeneration of the media with minimal impact in system downtime or astronaut involvement in overseeing the process.

The novel feature of this self-cleaning coatings approach is that this is an enabling technology that can actively, controllably, and reagentlessly regenerate filter media. The coatings application is amenable to industrial-scale manufacturing processes and should allow significantly increased useful lifetime for the filter media in an inexpensive fashion. The energy required to trigger the thermocycled self-cleaning is minimal, and can easily be diverted from heat exchange modules further downstream in the air revitalization system. The approach will further lower loads downstream in the air revitalization system, thereby contributing to increasing the lifetime of these modules, and decreasing the amount of replacement modules. These salient features will enable NASA to design more efficient and reliable, and less cumbersome,



Lynntech's **Self-Cleaning Coatings** technology for air filter media surfaces allows reagentless in-place regeneration of the surface.

some, air revitalization systems for future manned missions.

This work was done by Olivia Weber, Sanjiv Lalwani, and Anjal Sharma of Lynntech, Inc. for Glenn Research Center. Further information is contained in a TSP (see page 1).

Inquiries concerning rights for the commercial use of this invention should be addressed to NASA Glenn Research Center, Innovative Partnerships Office, Attn: Steven Fedor, Mail Stop 4-8, 21000 Brookpark Road, Cleveland, Ohio 44135. Refer to LEW-18848-1.



❁ Modular, Rapid Propellant Loading System/Cryogenic Testbed

John F. Kennedy Space Center, Florida

The Cryogenic Test Laboratory (CTL) at Kennedy Space Center (KSC) has designed, fabricated, and installed a modular, rapid propellant-loading system to simulate rapid loading of a launch-vehicle composite or standard cryogenic tank. The system will also function as a cryogenic testbed for testing and validating cryogenic innovations and ground support equipment (GSE) components. The modular skid-mounted system is capable of flow rates of liquid nitrogen from 1 to 900 gpm (≈ 3.8 to 3,400 L/min), of pressures from ambient to 225 psig (≈ 1.5 MPa), and of temperatures to -320 °F (≈ -195 °C). The system can be easily validated to flow liquid oxygen at a different location, and could be easily scaled to any particular vehicle interface requirements.

This innovation is the first phase of development of a smart Simulated Rapid Propellant Loading (SRPL) system that can be used at multiple sites for servicing multiple vehicle configurations with varying interface flow, temperature, and pressure requirements. The SRPL system can accommodate cryogenic components from $\frac{1}{4}$ to 8 in. (≈ 0.6 to 20 cm) and larger, and a variety of pneumatic component types and sizes. Temperature, pressure, flow, quality, and a variety of other sensors are also incorporated into the propellant system design along with the capability to adjust for the testing of a multitude of sensor types and sizes.

The system has three modules (skids) that can be placed at any launch vehicle site (or mobile), and can be connected with virtually any length of pipe re-

quired for a complete propellant loading system. The modules include a storage area pump skid (located near the storage tank and a dump basin), a valve control skid (located on or near the launch table to control flow to the vehicle, and to return to the tank or dump basin), and a vehicle interface skid (located at the vehicle). The skids are fully instrumented with pressure, temperature, flow, motor, pump controls, and data acquisition systems, and can be controlled from a control room, or locally from a PDA (personal digital assistant) or tablet PC.

This work was done by Walter Hatfield, Sr. and Kevin Jumper of ASRC Aerospace Corp. for Kennedy Space Center. Further information is contained in a TSP (see page 1). KSC-13460

❁ Compact, Low-Force, Low-Noise Linear Actuator

This actuator has potential uses in military and automotive applications.

NASA's Jet Propulsion Laboratory, Pasadena, California

Actuators are critical to all the robotic and manipulation mechanisms that are used in current and future NASA missions, and are also needed for many other industrial, aeronautical, and space activities. There are many types of actuators that were designed to operate as linear or rotary motors, but there is still a need for low-force, low-noise linear actuators for specialized applications, and the disclosed mechanism addresses this need.

A simpler implementation of a rotary actuator was developed where the end effector controls the motion of a brush for cleaning a thermal sensor. The mechanism uses a SMA (shape-memory alloy) wire for low force, and low noise. The linear implementation of the actuator incorporates a set of springs and mechanical hard-stops for resetting and fault tolerance to mechanical resistance. The actuator can be designed to work in a pull or push mode, or both. Depending on the volume envelope criteria, the actuator can be configured for scaling its

volume down to $4 \times 2 \times 1$ cm³. The actuator design has an inherent fault tolerance to mechanical resistance. The actuator has the flexibility of being designed for both linear and rotary motion. A specific configuration was designed and analyzed where fault-tolerant features have been implemented. In this configuration, an externally applied force larger than the design force does not damage the active components of the actuator. The actuator housing can be configured and produced using cost-effective methods such as injection molding, or alternatively, its components can be mounted directly on a small circuit board.

The actuator is driven by a SMA -NiTi as a primary active element, and it requires energy on the order of 20 Ws(J) per cycle. Electrical connections to points A and B are used to apply electrical power in the resistive NiTi wire, causing a phase change that contracts the wire on the order of 5%. The actuation period is of the order of a second for generating

the stroke, and 4 to 10 seconds for resetting. Thus, this design allows the actuator to work at a frequency of up to 0.1 Hz.

The actuator does not make use of the whole range of motion of the SMA material, allowing for large margins on the mechanical parameters of the design. The efficiency of the actuator is of the order of 10%, including the margins. The average dissipated power while driving at full speed is of the order of 1 W, and can be scaled down linearly if the rate of cycling is reduced. This design produces an extremely quiet actuator; it can generate a force greater than 2 N and a stroke greater than 1 cm. The operational duration of SMA materials is of the order of millions of cycles with some reduced stroke over a wide temperature range up to 150 °C.

This work was done by Mircea Badescu, Stewart Sherrit, and Yoseph Bar-Cohen of Caltech for NASA's Jet Propulsion Laboratory. Further information is contained in a TSP (see page 1). NPO-47991

Loop Heat Pipe With Thermal Control Valve as a Variable Thermal Link

New arrangement reduces energy demands while maintaining circuits and batteries within optimal temperature range.

Marshall Space Flight Center, Alabama

Future lunar landers and rovers will require variable thermal links that allow for heat rejection during the lunar daytime and passively prevent heat rejection during the lunar night. During the lunar day, the thermal management system must reject the waste heat from the electronics and batteries to maintain them below the maximum acceptable temperature. During the lunar night, the heat rejection system must either be shut down or significant amounts of guard heat must be added to keep the electronics and batteries above the minimum acceptable temperature. Since guard heater power is unfavorable because it adds to system size and complexity, a variable thermal link is preferred to limit heat removal from the electronics and batteries during the long lunar night. Conventional loop heat pipes (LHPs) can provide the required variable thermal conductance, but they still consume electrical power to shut down the heat transfer. This innovation adds a thermal control valve (TCV) and a bypass line to a conventional LHP that proportionally allows vapor to flow back into the compensation chamber of the LHP. The addition of this valve can achieve completely passive thermal control of the LHP, eliminating the need for guard heaters and complex controls.

A schematic of the system is shown in Figures 1 and 2 for operation during the Lunar day and night, respectively. During the Lunar day, maximum vapor flow to the radiator is desired for efficient operation. In the example shown, 95% of the vapor flows through the radiator and 5% flows through the bypass line. In contrast to the Lunar day, the thermal link must be as ineffective as possible during the Lunar night (see Figure 2). As the temperature of the TCV drops, more and more of the vapor is directed directly back into the compensation chamber, gradually shutting down the LHP.

Previous LHPs with a TCV have the bypass vapor flow directly mix with the liquid return line. In this arrangement, the vapor and liquid flows will interact with each other, possibly causing flow instabilities as the two streams come to the thermodynamic equilibrium. A LHP incorporating a passive TCV and bypass line proportionally allows vapor to flow back into the compensation chamber, minimizing flow instabilities experienced in previous LHPs with TCVs by allowing mixing of the vapor and liquid in the relatively large volume of the compensation chamber.

This work was done by John Hartenstine, William G. Anderson, Kara Walker, and Pete Dussinger of Advanced Cooling Technologies, Inc. for Marshall Space Flight Center. For more information, contact Sammy Nabors, MSFC Commercialization Assistance Lead, at sammy.a.nabors@nasa.gov. Refer to MFS-32915-1.

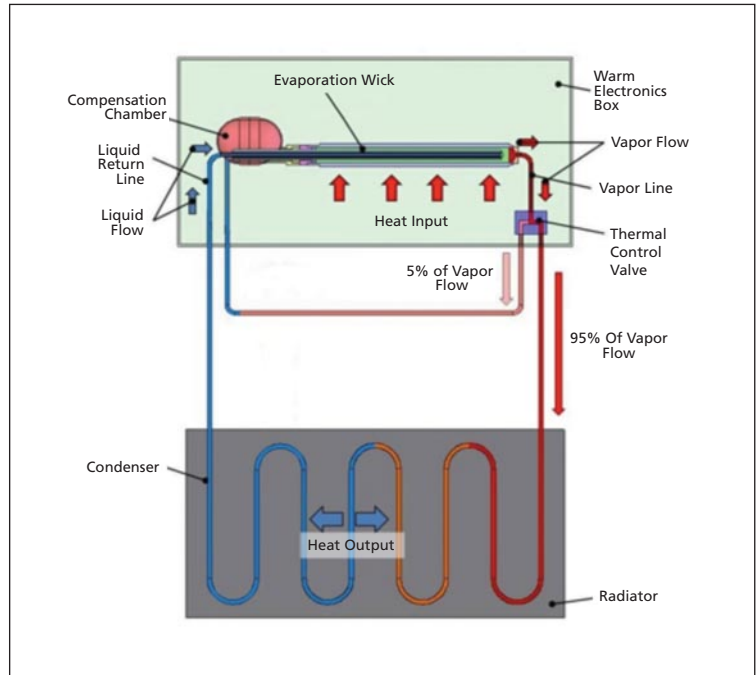


Figure 2. Variable Conductance Loop Heat Pipe schematic during the Lunar night. Most of the vapor flows directly back into the compensation chamber, shutting down the LHP. The 95% and 5% flow rates are representative.

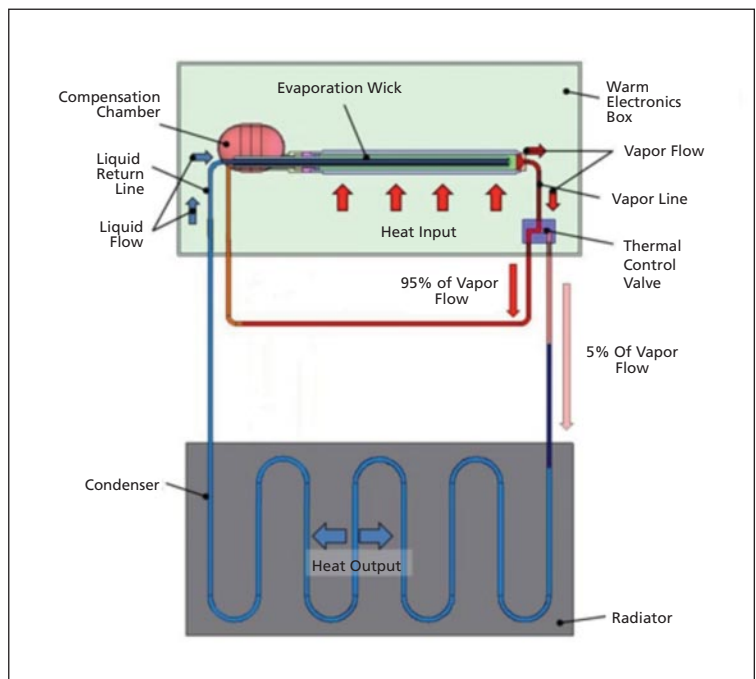


Figure 1. Variable Conductance Loop Heat Pipe schematic during the Lunar day. Most of the vapor flows through the radiator. The 5% and 95% flow rates are representative.

❁ Process for Measuring Over-Center Distances

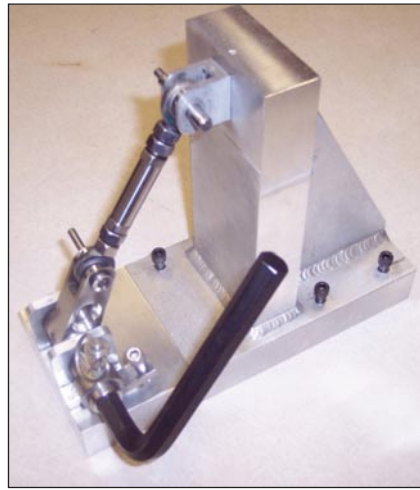
A more accurate approach enables mechanisms to be adjusted to within tight specifications.

John F. Kennedy Space Center, Florida

Over-center mechanisms were used in the orbiter payload bay to lock down the robotic arm during the launch of the space shuttle. These mechanisms were unlocked while in orbit in order to release the arm for use. Adjusting the mechanism such that it would not inadvertently release during launch, but could be released when needed by use of the motor, required accurate adjustments that were difficult to perform. A procedure was developed to allow these mechanisms to be adjusted to within the specifications required for the Space Shuttle Program. This approach is significantly more accurate than any other technique, and is the only technique known that met the launch requirements of the program.

Within the payload bay of the orbiters was a set of small over-center mechanisms that held the robotic arm in place. Each of these contained two straight segments connected with a pin. The upper end (called the driveline) was connected via a second pin to a hook, whose purpose was to hold the robotic arm securely in place until it was needed on a mission. The lower end (called the bellcrank) was connected to a gearbox via another pin or axle. In practice, this mechanism was adjusted such that the over-center pin could be forced through the on-line position a known over-center distance where the residual strain in the two straight segments would lock it in place (the stowed position). The distance and the force required had to be adjusted such that this mechanism would not deploy during launch, but such that a motor could drive the pin back through the on-line position to release the robotic arm when needed.

The problem was that the over-center distance was required to be set at 0.026-in. (≈ 0.7 mm), which was difficult to measure to the required accuracy [± 0.001 in. ($\approx \pm 0.03$ mm)]. Trying to find the on-line position, so that one could measure from it, was not possible be-



In this model of the **Over-Center Mechanism**, a hex wrench is used in place of the motor, but the rest of the components were machined to match those in the field.

cause the mechanism would only stay in this position if frictional forces held it, and these forces were directional and not consistent between measurements.

Some consideration was given to simply photographing the mechanism in its stowed position and measuring the distance between the center of the pin and a line connecting the centers of the outer two rotational pins, but this failed because the pin covers were not necessarily centered on the pin centers.

In order to understand the problem, a one-to-one scale model of the over-center mechanism was constructed (see figure). A hex wrench was used in place of the motor, but the rest of the components were machined to match those in the field. Several attempts at measuring the over-center position were attempted with this model, the first few of which failed. One of the advantages of having a model like this is that the dimensions of the parts were well known and the pins were all accessible, so the on-line position could be measured accurately using approaches not possible in the field.

A jig was constructed that used a depth gage to measure the distance to

the over-center pin while resting on the top and bottom pin. The hex wrench was replaced with a calibrated torque wrench. Then, the driveline (the upper half of the mechanism) was repositioned to make it difficult to push the device through the on-line position. Now, by applying a known torque, it was possible to measure a location to the center pin. Then, without changing the length of the driveline, the top pin was disconnected, the mechanism was placed into the stowed position, the top pin was reinserted, and the location of the center pin was measured while applying the opposite torque. In essence, this measured the location of the center pin while it was being pushed toward the on-line position from two different directions; the average of these two measurements was then the on-line position. Tests showed that this approach was accurate to ± 0.002 in. ($\approx \pm 0.05$ mm) where at least ± 0.001 in. ($\approx \pm 0.03$ mm) of error entered from the second measurement technique. Statistically, this new approach was accurate to ± 0.001 in. ($\approx \pm 0.03$ mm). Making static measurements, combined with working in regions where the strain is strongly dependent on position, led to this enhancement in measurement accuracy and solved the problem.

Because the prior method used an LDT (linear displacement transducer) and strain gauges, most of the necessary structures were already in place in the field to allow the new measurement process to be transferred. The depth gauge would be replaced by the LDT and the torque wrench by a wrench and a strain gauge. But rigid mounting brackets and a target (or contact point) were needed for the LDT in order to allow an accurate position measurement.

This work was done by Robert Youngquist and Douglas Willard of Kennedy Space Center, and Joddy Stahl, Kevin Murtland, and Steven Parks of ASRC Aerospace Corporation. Further information is contained in a TSP (see page 1). KSC-13212



Hands-Free Transcranial Color Doppler Probe

These probes enable full use of TCD technology for neurological diagnostics.

Lyndon B. Johnson Space Center, Houston, Texas

Current transcranial color Doppler (TCD) transducer probes are bulky and difficult to move in tiny increments to search and optimize TCD signals. This invention provides miniature motions of a TCD transducer probe to optimize TCD signals.

The mechanical probe uses a spherical bearing in guiding and locating the tilting crystal face. The lateral motion of the crystal face as it tilts across the full range of motion was achieved by minimizing the distance between the pivot location and the crystal face. The smallest commonly available metal spherical bearing was used with an outer diameter of 12 mm, a 3-mm tall retaining ring, and 5-mm overall height. Small geared motors were used that would provide sufficient power in a very compact package. After confirming the validity of the basic positioning concept, optimization design loops were completed to yield the final design.

A parallel motor configuration was used to minimize the amount of space wasted inside the probe case while minimizing the overall case dimensions. The distance from the front edge of the crys-

tal to the edge of the case was also minimized to allow positioning of the probe very close to the ear on the temporal lobe. The mechanical probe is able to achieve a $\pm 20^\circ$ tip and tilt with smooth repeatable action in a very compact package. The enclosed probe is about 7 cm long, 4 cm wide, and 1.8 cm tall.

The device is compact, hands-free, and can be adjusted via an innovative touchscreen. Positioning of the probe to the head is performed via conventional transducer gels and pillows. This device is amendable to having advanced software, which could intelligently focus and optimize the TCD signal.

The first effort will be development of monitoring systems for space use and field deployment. The need for long-lived, inexpensive clinical diagnostic instruments for military applications is substantial. Potential future uses of this system by NASA and other commercial end-users include monitoring cerebral blood flow of ambulatory patients, prognostic of potential for embolic stroke, ultrasonic blood clot treatment, monitoring open-heart and carotid end-

arterectomy surgery, and resolution of the controversy regarding transient ischemic attacks and emboli's role. Monitoring applications include those for embolism formation during diving ascents, changes in CBFV (cerebral blood flow velocity) in relation to cognitive function as associated with sick building syndrome or exposure to environmental and workplace toxins, changes of CBFV for testing and evaluating Gulf War Syndrome, and patients or subjects while moving or performing tasks.

This work was done by Robert Chin of GeneXpress Informatics, and Srihdar Madala and Graham Sattler of Indus Instruments for Johnson Space Center. Further information is contained in a TSP (see page 1).

In accordance with Public Law 96-517, the contractor has elected to retain title to this invention. Inquiries concerning rights for its commercial use should be addressed to:

*Indus Instruments
721 Tristar Drive, Suite C
Webster, TX 77598*

Refer to MSC-24702-1, volume and number of this NASA Tech Briefs issue, and the page number.

Improving Balance Function Using Low Levels of Electrical Stimulation of the Balance Organs

A device based on this technology may be used as a miniature patch worn by people with disabilities to improve posture and locomotion, and to enhance adaptability or skill acquisition.

Lyndon B. Johnson Space Center, Houston, Texas

Crewmembers returning from long-duration space flight face significant challenges due to the microgravity-induced inappropriate adaptations in balance/sensorimotor function. The Neuroscience Laboratory at JSC is developing a method based on stochastic resonance to enhance the brain's ability to detect signals from the balance organs of the inner ear and use them for rapid improvement in balance skill, especially when combined with balance training exercises. This method involves a stimulus delivery system that is

wearable/portable providing imperceptible electrical stimulation to the balance organs of the human body.

Stochastic resonance (SR) is a phenomenon whereby the response of a nonlinear system to a weak periodic input signal is optimized by the presence of a particular non-zero level of noise. This phenomenon of SR is based on the concept of maximizing the flow of information through a system by a non-zero level of noise. Application of imperceptible SR noise coupled with sensory input in hu-

mans has been shown to improve motor, cardiovascular, visual, hearing, and balance functions. SR increases contrast sensitivity and luminance detection; lowers the absolute threshold for tone detection in normal hearing individuals; improves homeostatic function in the human blood pressure regulatory system; improves noise-enhanced muscle spindle function; and improves detection of weak tactile stimuli using mechanical or electrical stimulation. SR noise has been shown to improve postural control when applied

as mechanical noise to the soles of the feet, or when applied as electrical noise at the knee and to the back muscles.

SR using imperceptible stochastic electrical stimulation of the vestibular system (stochastic vestibular stimulation, SVS) applied to normal subjects has shown to improve the degree of association between the weak input periodic signals introduced via venous blood pressure receptors and the heart-rate responses. Also, application of SVS over 24 hours improves the long-term heart-rate dynamics and motor responsiveness as

indicated by daytime trunk activity measurements in patients with multi-system atrophy, Parkinson's disease, or both, including patients who were unresponsive to standard therapy for Parkinson's disease. Recent studies conducted at the NASA JSC Neurosciences Laboratories showed that imperceptible SVS, when applied to normal, young, healthy subjects, leads to significantly improved balance performance during postural disturbances on unstable compliant surfaces. These studies have shown the benefit of SR noise characteristic opti-

mization with imperceptible SVS in the frequency range of 0–30 Hz, and amplitudes of stimulation have ranged from 100 to 400 microamperes.

This work was done by Jacob Bloomberg and Millard Reschke of Johnson Space Center; Ajitkumar Mulavara and Scott Wood of USRA; Jorge Serrador of Dept. of Veterans Affairs NJ Healthcare System; Matthew Fiedler, Igor Kofman, and Brian T. Peters of Wyle; and Helen Cohen of Baylor College. For further information, contact the JSC Innovation Partnerships Office at (281) 483-3809. MSC-25013-1

Developing Physiologic Models for Emergency Medical Procedures Under Microgravity

Lyndon B. Johnson Space Center, Houston, Texas

Several technological enhancements have been made to METI's commercial Emergency Care Simulator (ECS) with regard to how microgravity affects human physiology. The ECS uses both a software-only lung simulation, and an integrated mannequin lung that uses a physical lung bag for creating chest excursions, and a digital simulation of lung mechanics and gas exchange. METI's patient simulators incorporate models

of human physiology that simulate lung and chest wall mechanics, as well as pulmonary gas exchange.

Microgravity affects how O₂ and CO₂ are exchanged in the lungs. Procedures were also developed to take into account the Glasgow Coma Scale for determining levels of consciousness by varying the ECS eye-blinking function to partially indicate the level of consciousness of the patient. In addition, the ECS was modi-

fied to provide various levels of pulses from weak and thready to hyper-dynamic to assist in assessing patient conditions from the femoral, carotid, brachial, and pedal pulse locations.

This work was done by Nigel Parker and Veronica O'Quinn of Medical Education Tech, Inc. for Johnson Space Center. Further information is contained in a TSP (see page 1). MSC-23922-1

PMA-Linked Fluorescence for Rapid Detection of Viable Bacterial Endospores

This method has applications in the pharmaceutical, food microbiology, semiconductor, and other industries requiring surface sterilization.

NASA's Jet Propulsion Laboratory, Pasadena, California

The most common approach for assessing the abundance of viable bacterial endospores is the culture-based plating method. However, culture-based approaches are heavily biased and oftentimes incompatible with upstream sample processing strategies, which make viable cells/spores uncultivable. This shortcoming highlights the need for rapid molecular diagnostic tools to assess more accurately the abundance of viable spacecraft-associated microbiota, perhaps most importantly bacterial endospores.

Propidium monoazide (PMA) has received a great deal of attention due to its ability to differentiate live, viable

bacterial cells from dead ones. PMA gains access to the DNA of dead cells through compromised membranes. Once inside the cell, it intercalates and eventually covalently bonds with the double-helix structures upon photoactivation with visible light. The covalently bound DNA is significantly altered, and unavailable to downstream molecular-based manipulations and analyses. Microbiological samples can be treated with appropriate concentrations of PMA and exposed to visible light prior to undergoing total genomic DNA extraction, resulting in an extract comprised solely of DNA arising from viable cells. This ability to extract DNA

selectively from living cells is extremely powerful, and bears great relevance to many microbiological arenas.

While this PMA-based selective chemistry has been applied to several polymerase chain reaction (PCR)-based molecular protocols, it has never been coupled with fluorescence *in situ* hybridization (FISH)-based microscopic methods. FISH microscopy is a powerful technique for visualizing and enumerating microorganisms present in a given sample, which relies on the ability of fluorescently labeled oligonucleotide probes to gain access to, and hybridize with, specific nucleic acid sequences within cells. Dogmatic princi-

ples suggest that by first treating a sample with PMA and covalently modifying the DNA originating from dead cells, downstream FISH-based microscopy should then enable the direct, specific visualization and enumeration of only living, viable microorganisms. An effective and efficient coupling of PMA-based chemistry with downstream FISH-microscopic methods would significantly empower the current ability to discern viable from dead microbes by direct visualization.

The basic principle of this method is that PMA penetrates only the dead cells and/or spores, due to their compromised membrane structures. Once inside the cell, PMA strongly intercalates with DNA. PMA has a photoactive azide group that allows covalent cross-linkage to DNA upon exposure to bright white light. This photoactivation results in the formation of PMA-DNA complex that renders DNA inaccessible for hybridization reaction during FISH assay. To avoid the difficulties and problems associated with current methods for determining the actual numbers of living versus dead cellular entities examined, and biases associated therewith, a novel mo-

lecular-biological protocol was developed for selective detection and enumeration of viable microbial cells. After having been subjected to the procedures described herein, the viability (live vs. dead) of bacterial cells and spores could be discerned. Following treatment with PMA, living, viable cells and spores were shown to be receptive to fluorescently labeled oligonucleotide probes, as hybridization and FISH-based microscopy was successful. Dead cells and spores, however, were not detected, as the pretreatment with PMA rendered their DNA unavailable to hybridization with the FISH-probes.

The true novelty of the technology is the coupling of a downstream, highly specific means of visualizing microbial cells and spores with a chemical pretreatment that precludes the portion of the microbial consortium that is not living (non-viable) from being detected. This results in the ability to selectively visualize and enumerate only the living cells and spores present in a given sample, in a molecular biological fashion, without the need for heavily biased cultivation-based methodologies. This novel study demonstrates that PMA penetrates

only the heat-killed spores, which precludes downstream hybridization reactions in the FISH assay. This novel PMA-FISH method is an attractive tool to detect viable endospores in spacecraft-associated environments, which is of crucial importance and benefit to planetary protection practices aimed at reducing the abundance of spacecraft-borne microbial contaminants.

This work was done by Myron T. La Duc and Kasthuri Venkateswaran of Caltech, and Bidyut Mohapatra of the University of South Alabama for NASA's Jet Propulsion Laboratory. For more information, contact iaoffice@jpl.nasa.gov.

In accordance with Public Law 96-517, the contractor has elected to retain title to this invention. Inquiries concerning rights for its commercial use should be addressed to:

*Innovative Technology Assets Management
JPL*

Mail Stop 202-233

4800 Oak Grove Drive

Pasadena, CA 91109-8099

E-mail: iaoffice@jpl.nasa.gov

Refer to NPO-48040, volume and number of this NASA Tech Briefs issue, and the page number.

Portable Intravenous Fluid Production Device for Ground Use

This small, portable device with high output produces medical injection-grade sterile water from potable water sources.

John F. Kennedy Space Center, Florida

There are several medical conditions that require intravenous (IV) fluids. Limitations of mass, volume, storage space, shelf-life, transportation, and local resources can restrict the availability of such important fluids. These limitations are expected in long-duration space exploration missions and in remote or austere environments on Earth. Current IV fluid production requires large factory-based processes. Easy, portable, on-site production of IV fluids can eliminate these limitations. Based on experience gained in developing a device for spaceflight, a ground-use device was developed.

This design uses regular drinking water that is pumped through two filters to produce, in minutes, sterile, ultrapure water that meets the stringent quality standards of the United States Pharmacopeia for Water for Injection (Total Bacteria, Conductivity, Endo-

toxins, Total Organic Carbon). The device weighs 2.2 lb (1 kg) and is 10 in. long, 5 in. wide, and 3 in. high (≈25, 13, and 7.5 cm, respectively) in its storage configuration. This handheld device produces one liter of medical-grade water in 21 minutes. Total production capacity for this innovation is expected to be in the hundreds of liters.

The device contains one battery powered electric mini-pump. Alternatively, a manually powered pump can be attached and used. Drinking water enters the device from a source water bag, flows through two filters, and final sterile production water exits into a sealed, medical-grade collection bag. The collection bag contains pre-placed crystalline salts to mix with product water to form isotonic intravenous medical solutions. Alternatively, a hypertonic salt solution can be injected into a filled bag. The filled collection bag is de-

tached from the device and is ready for use or storage. This device currently contains one collection bag, but a manifold of several pre-attached bags or replacement of single collection bags under sterile needle technique is possible for the production of multiple liters. The entire system will be flushed, sealed, and radiation-sterilized.

Operation of the device is easy and requires minimal training. Drinking water is placed into the collection bag. Inline stopcock flow valves at the source and collection bags are opened, and the mini-pump is turned on by a switch to begin fluid flow. When the collection bag is completely filled with the medical-grade water, the pump can be turned off. The pump is designed so it cannot pump air, and overfilling of the collection bag with fluid is avoided by placing an equal amount of water in the source bag. Backflow is avoided by in-

line check valves. The filled collection bag is disconnected from its tubing and is ready for use. The source bag can be refilled for production of multiple liters, or the source bag can be replaced with an input tube that can be placed in a larger potable water source if the device is attended. The device functions in all orientations independent of any gravity fields.

In addition to creating IV fluids, the device produces medical-grade water, which can be used for mixing with medications for injection, reconstituting freeze-dried blood products for injection, or for wound hydration or irrigation.

Potential worldwide use is expected with medical activities in environments that have limited resources, storage, or resupply such as in military field opera-

tions, humanitarian relief efforts, submarines, commercial cruise ships, etc.

This work was done by Philip J. Scarpa of Kennedy Space Center and Wolfgang K. Scheuer of Tiger Purification Systems, Inc. For more information, contact Dr. Philip Scarpa at (321) 867-6386 or Philip.J.Scarpa@nasa.gov. KSC-13598

Adaptation of a Filter Assembly to Assess Microbial Bioburden of Pressurant Within a Propulsion System

NASA's Jet Propulsion Laboratory, Pasadena, California

A report describes an adaptation of a filter assembly to enable it to be used to filter out microorganisms from a propulsion system. The filter assembly has previously been used for particulates $>2\ \mu\text{m}$. Projects that utilize large volumes of nonmetallic materials of planetary protection concern pose a challenge to their bioburden budget, as a conservative specification value of $30\ \text{spores}/\text{cm}^3$ is typically used.

Helium was collected utilizing an adapted filtration approach employing

an existing Millipore filter assembly apparatus used by the propulsion team for particulate analysis. The filter holder on the assembly has a 47-mm diameter, and typically a $1.2\text{--}5\ \mu\text{m}$ pore-size filter is used for particulate analysis making it compatible with commercially available sterilization filters ($0.22\ \mu\text{m}$) that are necessary for biological sampling.

This adaptation to an existing technology provides a proof-of-concept and a demonstration of successful use in a ground equipment system. This adapta-

tion has demonstrated that the Millipore filter assembly can be utilized to filter out microorganisms from a propulsion system, whereas in previous uses the filter assembly was utilized for particulates $>2\ \mu\text{m}$.

This work was done by James N. Benardini, Robert C. Koukol, Wayne W. Schubert, Fabian Morales, and Martin F. Klatte of Caltech for NASA's Jet Propulsion Laboratory. Further information is contained in a TSP (see page 1). NPO-48304



Multiplexed Force and Deflection Sensing Shell Membranes for Robotic Manipulators

This technology can be used to enhance precision in robotic surgery.

Lyndon B. Johnson Space Center, Houston, Texas

Force sensing is an essential requirement for dexterous robot manipulation, e.g., for extravehicular robots making vehicle repairs. Although strain gauges have been widely used, a new sensing approach is desirable for applications that require greater robustness, design flexibility including a high degree of multiplexibility, and immunity to electromagnetic noise.

This invention is a force and deflection sensor — a flexible shell formed with an elastomer having passageways formed by apertures in the shell, with an optical fiber having one or more Bragg gratings positioned in the passageways for the measurement of force and deflection.

One object of the invention is lightweight, rugged appendages for a robot that feature embedded sensors so that the robot can be more “aware” of loads in real time. A particular class of optical sensors, fiber Bragg grating (FBG) sensors, is promising for space robotics and other applications where high sensitivity, multiplexing capability, immunity to electromagnetic noise, small size, and resistance to harsh environments are particularly desirable. In addition, the biosafe and inert nature of optical fibers makes them attractive for medical robotics. FBGs reflect light with a peak wavelength that shifts in proportion to the strain to which they are subjected.

Multiple FBG sensors can be placed along a single fiber and optically multiplexed. FBG sensors have previously been surface-attached to or embedded in metal parts and composites to monitor stresses.

An exoskeletal force sensing robot finger was developed by embedding FBG sensors into a polymer-based structure. Multiple FBG sensors were embedded into the structure to allow the manipulator to sense and measure both contact forces and grasping forces. In order to fabricate a three-dimensional structure, a new shape deposition manufacturing (SDM) process was developed. The sensorized SDM-fabricated finger was then characterized using an FBG interrogator. A force localization scheme was also developed.

A sensor is formed from a thin shell of flexible material such as elastomer to form an attachment region, a sensing region, and a tip region. In one embodiment, the sensing region is a substantially cylindrical flexible shell, and has a plurality of apertures forming passageways between the apertures. Optical fiber is routed through the passageways, with sensors located in the passageways prior to the application of the elastomeric material forming the flexible shell. Deflection of the sensor, such as by a force applied to the contact region, causes an incremental strain in one or

more passageways where the optical fiber is located. The incremental strain results in a change of optical wavelength of reflection or transmittance at the sensor, thereby allowing the measurement of force or displacement.

The ability to route a single optical fiber through the passageways of the outer shell of the sensor, combined with the freedom to place Bragg grating-based sensors in desired locations of the shell, provides tremendous flexibility in sensing force in three axes, as well as the possibility of providing a large number of sensors for more sophisticated measurement modalities, such as torque and shell deflection in response to multi-point pressure application.

This work was done by Yong-Lae Park, Richard Black, Behzad Moslehi, Mark Cutkosky, and Kelvin Chau of Intelligent Fiber Optic Systems Corp. for Johnson Space Center. Further information is contained in a TSP (see page 1).

In accordance with Public Law 96-517, the contractor has elected to retain title to this invention. Inquiries concerning rights for its commercial use should be addressed to:

*Intelligent Fiber Optic Systems Corp.
424 Panama Mall
Stanford, CA 94305*

Refer to MSC-24501-1, volume and number of this NASA Tech Briefs issue, and the page number.

Whispering Gallery Mode Optomechanical Resonator

These devices can be used for remote and inertial sensing, and mass detection.

NASA's Jet Propulsion Laboratory, Pasadena, California

Great progress has been made in both micromechanical resonators and micro-optical resonators over the past decade, and a new field has recently emerged combining these mechanical and optical systems. In such optomechanical systems, the two resonators are

strongly coupled with one influencing the other, and their interaction can yield detectable optical signals that are highly sensitive to the mechanical motion. A particularly high- Q optical system is the whispering gallery mode (WGM) resonator, which has many ap-

plications ranging from stable oscillators to inertial sensor devices. There is, however, limited coupling between the optical mode and the resonator's external environment. In order to overcome this limitation, a novel type of optomechanical sensor has been developed, of-

fering great potential for measurements of displacement, acceleration, and mass sensitivity.

The proposed hybrid device combines the advantages of all-solid optical WGM resonators with high-quality micro-machined cantilevers. For direct access to the WGM inside the resonator, the idea is to radially cut precise gaps into the perimeter, fabricating a mechanical resonator within the WGM. Also, a strategy to reduce losses has been developed with optimized design of the cantilever geometry and positions of gap surfaces.

The cantilever is machined by making fine cuts in a high- Q crystalline WGM resonator using focused ion-beam (FIB) technology. Such cuts can be much smaller than the optical wavelength, which should preserve the quality of the optical resonator. At the same time, reflection from the cantilever surfaces will result in coupling between the degenerate clockwise and

counterclockwise propagating WGM. Therefore, a well-established technique of position-sensitive, dual-resonator coupling will be implemented in a novel system with optical and mechanical resonators' high quality factors. This technique allows for optical cooling, as well as heating, of the mechanical oscillator.

This innovative hybrid system combines the advantages of both WGM and Fabry-Perot (FP) cavity resonators by utilizing the WGM resonator with the aforementioned cuts in the crystal to create an independent micromechanical resonator, residing directly in the middle of the optical WGM as an integral structure of the disk. This feature allows the direct coupling of the mechanical motion to the optical modes, much like a membrane inside an FP cavity. In this configuration, the single-mode optomechanical interaction can be selectively accessed as with a standard WGM resonator, or the coupled

optical mode interaction as in that of a membrane-FP cavity.

The challenge of this approach is to maintain the optical finesse in the presence of the air gaps and the corresponding interfaces. The partially reflecting surfaces result in standing waves (SWs) in the resonators, and the mode coupling between them. These interfaces can also introduce scattering and diffraction losses. The estimates and previous WGM experiments suggest that a combination of appropriate microfabrication processes, such as FIB, and strategic use of SW modes, can reduce the losses and yield an optical resonator $Q \approx 10^8$, higher than any cavity Q of optomechanical systems at the time of this reporting.

This work was done by David C. Aveline, Dmitry V. Strelakov, Nan Yu, and Karl Y. Yee of Caltech for NASA's Jet Propulsion Laboratory. Further information is contained in a TSP (see page 1). NPO-47114

Vision-Aided Autonomous Landing and Ingress of Micro Aerial Vehicles

This technology enables a micro aerial vehicle to transition autonomously between indoor and outdoor environments via windows and doors based on monocular vision.

NASA's Jet Propulsion Laboratory, Pasadena, California

Micro aerial vehicles have limited sensor suites and computational power. For reconnaissance tasks and to conserve energy, these systems need the ability to autonomously land at vantage points or enter buildings (ingress). But for autonomous navigation, information is needed to identify and guide the vehicle to the target. Vision algorithms can provide egomotion estimation and target detection using input from cameras that are easy to include in miniature systems.

Target detection based on visual feature tracking and planar homography decomposition is used to identify a target for automated landing or building ingress, and to produce 3D waypoints to locate the navigation target. The vehicle control algorithm collects these waypoints and estimates the accurate target position to perform automated maneuvers for autonomous landing or building ingress.

Systems that are deployed outdoors can overcome this issue by using GPS

data for pose recovery, but this is not an option for systems operating in deep space or indoors. To cope with this issue, a system was developed on a small unmanned aerial vehicle (UAV) platform with a minimal sensor suite that can operate using only onboard resources to autonomously achieve basic navigation tasks. As a first step towards this goal, a navigation approach was developed that visually detects and reconstructs the position of navigation targets, but depends on an external VICON tracking system to regain scale and for closed-loop control.

A method was demonstrated of vision-aided autonomous navigation of a micro aerial vehicle with a single monocular camera, considering two different example applications in urban environments: autonomous landing on an elevated surface and automated building ingress. The method requires no special preparation (labels or markers) of the landing or ingress locations. Rather, leveraging the planar character of urban structure,

the vision system uses a planar homography decomposition to detect navigation targets and produce approach waypoints as an input to the vehicle control algorithm. Scale recovery is achieved using motion capture data. A real-time implementation running onboard a micro aerial vehicle was demonstrated in experimental runs.

The system is able to generate highly accurate target waypoints. Using a three-stage control scheme, one is able to autonomously detect, approach, and land on an elevated landing surface that is only slightly larger than the footprint of the aerial vehicles, and gather navigation target waypoints for building ingress. All algorithms run onboard the vehicles.

This work was done by Roland Brockers, Jeremy C. Ma, and Larry H. Matthies of Caltech; and Patrick Bouffard of the University of California, Berkeley for NASA's Jet Propulsion Laboratory. For more information, contact iaoffice@jpl.nasa.gov. NPO-47841

Self-Sealing Wet Chemistry Cell for Field Analysis

Analysis of soluble species in field samples is required in agriculture, soil science, and biomedical applications.

NASA's Jet Propulsion Laboratory, Pasadena, California

In most analytical investigations, there is a need to process complex field samples for the unique detection of analytes, especially when detecting low-concentration organic molecules that may identify extraterrestrial life. Wet chemistry based instruments are the techniques of choice for most laboratory-based analysis of organic molecules due to several factors including less fragmentation of fragile biomarkers, and ability to concentrate target species resulting in much lower limits of detection. Development of an automated wet chemistry preparation system that can operate autonomously on Earth and is also designed to operate under Martian ambient conditions will demonstrate the technical feasibility of including wet chemistry on future missions. An Automated Sample Processing System (ASPS) has recently been developed that receives fines, extracts organics through solvent extraction, processes the extract by removing non-organic soluble species, and delivers sample to multiple instruments for analysis

(including for non-organic soluble species). The key to this system is a sample cell that can autonomously function under field conditions.

As a result, a self-sealing sample cell was developed that can autonomously hermetically seal fines and powder into a container, regardless of orientation of the apparatus. The cap is designed with a beveled edge, which allows the cap to be self-righted as the capping motor engages. Each cap consists of a C-clip lock ring below a crucible O-ring that is placed into a groove cut into the sample cap. As the capping motor pushes the cap down onto the cell, the lock ring engages a small groove cut into the cell body. When the C-clip engages, the cap locks onto the sample cell. The seal is created through the O-ring, which is pushed down the body of the cell, resulting in a clean seal that has not leaked during multiple tests with 2,000 psi (≈ 13.8 MPa) of pressure.

The sample cells allow solvent to be inserted into the cell through a high-pressure check valve at the bottom of the cell.

The spring-loaded back end also comes with a 5- μ m sintered metal filter that removes particulates as the solvent and analyte are removed from the cell and delivered to the analytical instrumentation for analysis. Additionally, the check valve is nominally closed so that any residual solvent remains in the cell and does not contaminate other instruments.

This type of technique is vital for *in situ* chemical analysis on future flight missions. The current commercial benchtop model that performs this type of operation weighs well over 60 kg, and needs to be loaded by hand, including a consumable filter. The new cells are completely reusable with the only consumables being a C-clip and two O-rings, and have been demonstrated to be reusable over 50 times in laboratory testing.

This work was done by Luther W. Beegle of Caltech, and Juancarlos Soto, James Lasnik, and Shane Roark of Ball Aerospace & Technologies Corp. for NASA's Jet Propulsion Laboratory. For more information, contact iaoffice@jpl.nasa.gov. NPO-47977



General MACOS Interface for Modeling and Analysis for Controlled Optical Systems

NASA's Jet Propulsion Laboratory, Pasadena, California

The General MACOS Interface (GMI) for Modeling and Analysis for Controlled Optical Systems (MACOS) enables the use of MATLAB as a front-end for JPL's critical optical modeling package, MACOS. MACOS is JPL's in-house optical modeling software, which has proven to be a superb tool for advanced systems engineering of optical systems. GMI, coupled with MACOS, allows for seamless interfacing with modeling tools from other disciplines to make possible integration of dynamics, structures, and thermal models with the addition of control systems for deformable optics and other actuated optics.

This software package is designed as a tool for analysts to quickly and easily use MACOS without needing to be an expert at programming MACOS. The strength of MACOS is its ability to interface with various modeling/development platforms, allowing evaluation of system performance with thermal, mechanical, and optical modeling parameter variations. GMI provides an improved means for accessing selected key MACOS functionalities. The main objective of GMI is to marry the vast mathematical and graphical capabilities of MATLAB with the powerful optical analysis engine of MACOS, thereby pro-

viding a useful tool to anyone who can program in MATLAB. GMI also improves modeling efficiency by eliminating the need to write an interface function for each task/project, reducing error sources, speeding up user/modeling tasks, and making MACOS well suited for fast prototyping.

This work was done by Norbert Sigrist, Scott A. Basinger, and David C. Redding of Caltech for NASA's Jet Propulsion Laboratory. For more information, contact iaoffice@jpl.nasa.gov.

This software is available for commercial licensing. Please contact Daniel Broderick of the California Institute of Technology at danielb@caltech.edu. Refer to NPO-48009.



Books & Reports

Mars Technology Rover with Arm-Mounted Percussive Coring Tool, Microimager, and Sample-Handling Encapsulation Containerization Subsystem

A report describes the PLuto (programmable logic) Mars Technology Rover, a mid-sized FIDO (field integrated design and operations) class rover with six fully drivable and steerable cleated wheels, a rocker-bogey suspension, a pan-tilt mast with panorama and navigation stereo camera pairs, forward and rear stereo hazcam pairs, internal avionics with motor drivers and CPU, and a 5-degrees-of-freedom robotic arm.

The technology rover was integrated with an arm-mounted percussive coring tool, microimager, and sample handling encapsulation containerization subsystem (SHEC). The turret of the arm contains a percussive coring drill and microimager. The SHEC sample caching system mounted to the rover body contains coring bits, sample tubes, and sample plugs.

The coring activities performed in the field provide valuable data on drilling

conditions for NASA tasks developing and studying coring technology. Caching of samples using the SHEC system provide insight to NASA tasks investigating techniques to store core samples in the future.

This work was done by Paulo J. Younse, Matthew A. Diccio, and Albert R. Morgan of Caltech for NASA's Jet Propulsion Laboratory. Further information is contained in a TSP (see page 1). NPO-47917

Fault-Tolerant, Real-Time, Multi-Core Computer System

A document discusses a fault-tolerant, self-aware, low-power, multi-core computer for space missions with thousands of simple cores, achieving speed through concurrency. The proposed machine decides how to achieve concurrency in real time, rather than depending on programmers. The driving features of the system are simple hardware that is modular in the extreme, with no shared memory, and software with significant runtime reorganizing capability.

The document describes a mechanism for moving ongoing computations

and data that is based on a functional model of execution. Because there is no shared memory, the processor connects to its neighbors through a high-speed data link. Messages are sent to a neighbor switch, which in turn forwards that message on to its neighbor until reaching the intended destination. Except for the neighbor connections, processors are isolated and independent of each other.

The processors on the periphery also connect chip-to-chip, thus building up a large processor net. There is no particular topology to the larger net, as a function at each processor allows it to forward a message in the correct direction. Some chip-to-chip connections are not necessarily nearest neighbors, providing short cuts for some of the longer physical distances. The peripheral processors also provide the connections to sensors, actuators, radios, science instruments, and other devices with which the computer system interacts.

This work was done by Kim P. Gostelow of Caltech for NASA's Jet Propulsion Laboratory. Further information is contained in a TSP (see page 1). NPO-47894



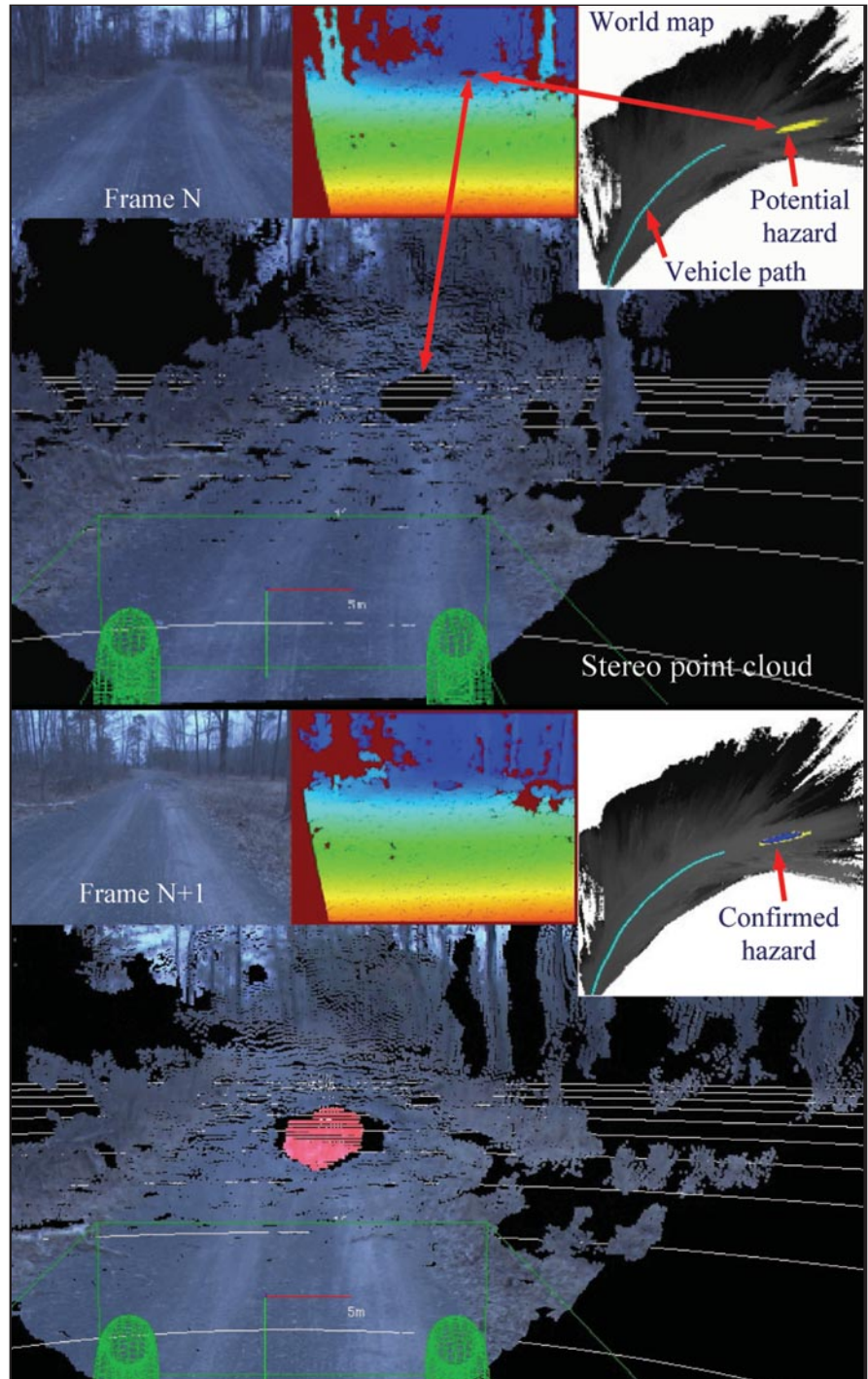
Water Detection Based on Object Reflections

NASA's Jet Propulsion Laboratory, Pasadena, California

Water bodies are challenging terrain hazards for terrestrial unmanned ground vehicles (UGVs) for several reasons. Traversing through deep water bodies could cause costly damage to the electronics of UGVs. Additionally, a UGV that is either broken down due to water damage or becomes stuck in a water body during an autonomous operation will require rescue, potentially drawing critical resources away from the primary operation and increasing the operation cost. Thus, robust water detection is a critical perception requirement for UGV autonomous navigation.

One of the properties useful for detecting still water bodies is that their surface acts as a horizontal mirror at high incidence angles. Still water bodies in wide-open areas can be detected by geometrically locating the exact pixels in the sky that are reflecting on candidate water pixels on the ground, predicting if ground pixels are water based on color similarity to the sky and local terrain features. But in cluttered areas where reflections of objects in the background dominate the appearance of the surface of still water bodies, detection based on sky reflections is of marginal value. Specifically, this software attempts to solve the problem of detecting still water bodies on cross-country terrain in cluttered areas at low cost.

Still water bodies are indirectly detected in cluttered areas of cross-country terrain by detecting reflections of objects in the water bodies using imagery acquired from a stereo pair of color cameras, which are mounted to the front of a terrestrial UGV. Object reflections can be from naturally occurring (e.g. vegetation, trees, hills, mountains, clouds) or man-made entities (e.g. signs, poles, vehicles, buildings, bridges). Color cameras provide a lower-cost solution than specialized imaging sensors (such as a polarization camera) and laser scanners. In addition, object reflections can be detected in water bodies with stereo vision at further ranges than with lidar scanners.



A hole in **Stereo Range Data** may be a water body still too small to be detected in image space. In this example, the hole was labeled a potential hazard in the world map in frame N. In the next frame, where there was previously a hole, there was range data that was detected as an object reflection, providing confirmation of a water body.

Four methods for detecting object reflections have been implemented: detection in the rectified camera images using cross correlation, detection in stereo range images, detection in a world map generated from range data, and detection using combined stereo range images and rectified camera images. Detection in stereo range images (see figure) exploits the knowledge that 3D coordinates of stereo range data on object reflections occur below the ground surface at a range close to that of the reflecting object.

Any autonomous robotic platform used on cross-country terrain that has restrictions on driving through water could benefit from this software, including military platforms and perhaps some agricultural platforms. The automotive industry could potentially benefit from an application of this technology to detect wet pavement.

This work was done by Arturo L. Rankin and Larry H. Matthies of Caltech for NASA's Jet Propulsion Laboratory. Further information is contained in a TSP (see page 1).

In accordance with Public Law 96-517, the contractor has elected to retain title to this invention. Inquiries concerning rights for its commercial use should be addressed to:

*Innovative Technology Assets Management
JPL*

Mail Stop 202-233

4800 Oak Grove Drive

Pasadena, CA 91109-8099

E-mail: iaoffice@jpl.nasa.gov

Refer to NPO-48494, volume and number of this NASA Tech Briefs issue, and the page number.

SATPLOT for Analysis of SECCHI Heliospheric Imager Data

NASA's Jet Propulsion Laboratory, Pasadena, California

Determining trajectories of solar transients such as coronal mass ejections is not always easy. White light images from SECCHI's (Sun Earth Connection Coronal and Heliospheric Investigation) heliospheric imagers are difficult to interpret because they represent a line-of-sight projection of optically thin solar wind structures. A structure's image by itself gives no information about its angle of propagation relative to the Sun-spacecraft line, and an image may show a superposition of several structures, all propagating at different angles. Analyzing SECCHI heliospheric imager data using plots of elongation (angle from the

Sun) versus time at fixed position angle (aka "Jplots") has proved extremely useful in understanding the observed solar wind structures. This technique has been used to study CME (coronal mass ejection) propagation, CIRs (corotating interaction regions), and blobs.

SATPLOT software was developed to create and analyze such elongation versus time plots. The tool uses a library of cylindrical maps of the data for each spacecraft's panoramic field-of-view. Each map includes data from three SECCHI white-light telescopes (the COR2 coronagraph and both heliospheric imagers) at one time for one spacecraft.

The maps are created using a Plate Carree projection, optimized for creating the elongation versus time plots. The tool can be used to analyze the observed tracks of features seen in the maps, and the tracks are then used to extract information, for example, on the angle of propagation of the feature.

This work was done by Jeffrey R. Hall and Paulett C. Liewer of Caltech for NASA's Jet Propulsion Laboratory. Further information is contained in a TSP (see page 1).

This software is available for commercial licensing. Please contact Daniel Broderick of the California Institute of Technology at danielb@caltech.edu. Refer to NPO-47826.

Plug-in Plan Tool v3.0.3.1

Lyndon B. Johnson Space Center, Houston, Texas

The role of PLUTO (Plug-in Port Utilization Officer) and the growth of the International Space Station (ISS) have exceeded the capabilities of the current tool PiP (Plug-in Plan). Its users (crew and flight controllers) have expressed an interest in a new, easy-to-use tool with a higher level of interactivity and functionality that is not bound by the limitations of Excel.

The PiP Tool assists crewmembers and ground controllers in making real-time decisions concerning the safety and compatibility of hardware plugged into the UOPs (Utility Outlet Panels) onboard the ISS. The PiP Tool also provides a reference to the current configuration of the hardware plugged in to the

UOPs, and enables the PLUTO and crew to test Plug-in locations for constraint violations (such as cable connector mismatches or amp limit violations), to see the amps and volts for an end item, to see whether or not the end item uses 1553 data, and the cable length between the outlet and the end item. As new equipment is flown or returned, the database can be updated appropriately as needed. The current tool is a macro-heavy Excel spreadsheet with its own database and reporting functionality.

The new tool captures the capabilities of the original tool, ports them to new software, defines a new dataset, and compensates for ever-growing unique constraints associated with the

Plug-in Plan. New constraints were designed into the tool, and updates to existing constraints were added to provide more flexibility and customizability. In addition, there is an option to associate a "Flag" with each device that will let the user know there is a unique constraint associated with it when they use it. This helps improve the safety and efficiency of real-time calls by limiting the amount of "corporate knowledge" overhead that has to be trained and learned through use.

The tool helps save time by automating previous manual processes, such as calculating connector types and deciding which cables are required and in what order.

This project provides a better onboard tool for the crew to safely test ideas for reconfigurations before calling the ground, and send the changes directly. The layout provides clear detail for power channels, module locations, and data ports, and allows for intuitive “drag-and-drop” connections from the database. The software will allow only com-

patible connections to occur, and will flag violations if they exist. It also allows the user to flag unique constraints that might not be caught by the software’s existing rules and calculations.

The PiP Tool includes reporting capabilities that allow the user to export database information and configuration information to Excel to share with others

or run detailed comparisons and searches as needed.

This work was done by Kathleen E. Andrea-Liner, Brion J. Au, Blake R. Fisher, Watchara Rodbumrung, Jeffrey C. Hamic, Kary Smith, and David S. Beadle of the United Space Alliance for Johnson Space Center. Further information is contained in a TSP (see page 1). MSC-24872-1

Frequency Correction for MIRO Chirp Transformation Spectroscopy Spectrum

NASA’s Jet Propulsion Laboratory, Pasadena, California

This software processes the flyby spectra of the Chirp Transform Spectrometer (CTS) of the Microwave Instrument for Rosetta Orbiter (MIRO). The tool corrects the effect of Doppler shift and local-oscillator (LO) frequency shift during the flyby mode of MIRO operations. The frequency correction for CTS flyby spectra is performed and is integrated with multiple spectra into a high signal-to-noise averaged spectrum at the rest-frame RF frequency. This innovation also generates the 8 molecular line spectra by dividing continuous 4,096-channel CTS spectra. The 8 line spectra can then be readily used for scientific investigations.

A spectral line that is at its rest frequency in the frame of the Earth or an asteroid will be observed with a time-varying Doppler shift as seen by MIRO. The frequency shift is toward the higher RF frequencies on approach, and toward lower RF frequencies on departure. The magnitude of the shift depends on the flyby velocity. The result of time-varying Doppler shift is that of an observed spectral line will be seen to move from channel to channel in the CTS spectrometer. The direction (higher or lower frequency) in the spectrometer depends on the spectral line frequency under consideration. In order to analyze the flyby spectra, two

steps are required. First, individual spectra must be corrected for the Doppler shift so that individual spectra can be superimposed at the same rest frequency for integration purposes. Second, a correction needs to be applied to the CTS spectra to account for the LO frequency shifts that are applied to asteroid mode.

This work was done by Seungwon Lee of Caltech for NASA’s Jet Propulsion Laboratory. Further information is contained in a TSP (see page 1).

This software is available for commercial licensing. Please contact Daniel Broderick of the California Institute of Technology at danielb@caltech.edu. Refer to NPO-47304.

Nonlinear Estimation Approach to Real-Time Georegistration from Aerial Images

This technology can be used for real-time search and rescue operations and surveillance applications using cameras mounted on aircraft or UAVs.

NASA’s Jet Propulsion Laboratory, Pasadena, California

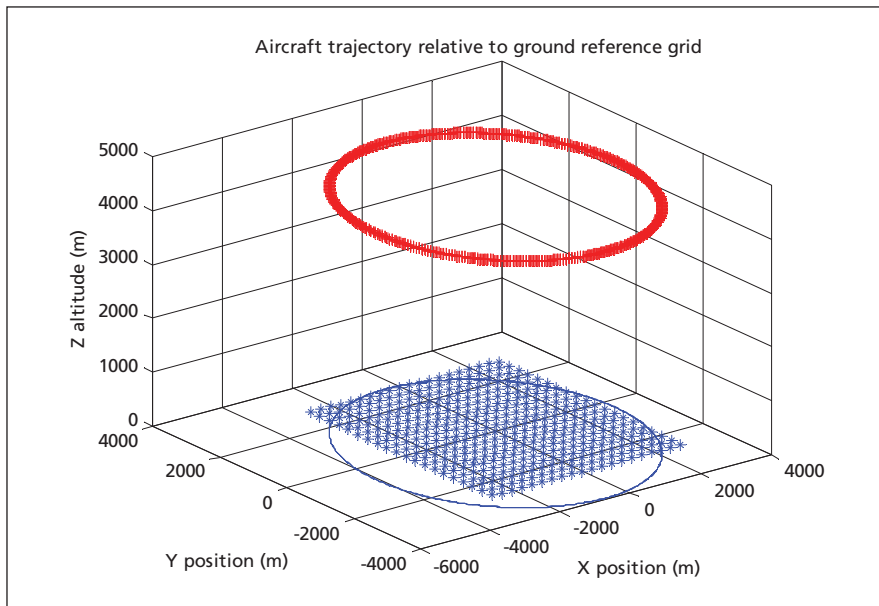
When taking aerial images, it is important to know locations of specific points of interest in an Earth-centered coordinate system (latitude, longitude, height) (see figure). The correspondence between a pixel location in the image and its Earth coordinate is known as georegistration. There are two main technical challenges arising in the intended application. The first is that no known features are assumed to be available in any of the images. The second is that the intended applications are real time. Here, images are taken at regular intervals (i.e. once per second), and it is desired to make decisions in real time based on the

geolocation of specific objects seen in the images as they arrive. This is in sharp contrast to most current methods for geolocation that operate “after-the-fact” by processing, on the ground, a database of stored images using computationally intensive methods.

The solution is a nonlinear estimation algorithm that combines processed real-time camera images with vehicle position and attitude information obtained from an onboard GPS receiver. This approach provides accurate georegistration estimates (latitude, longitude, height) of arbitrary features and/or points of interest seen in the camera im-

ages. This solves the georegistration problem at the modest cost of augmenting the camera information with a GPS receiver carried onboard the vehicle.

The nonlinear estimation algorithm is based on a linearized Kalman filter structure that carries 19 states in its current implementation. Six of the 19 states are calibration parameters associated with the initial camera pose. One of the states calibrates the scale factor associated with all camera-derived information. The remaining 12 states are used to model the current kinematic state of the vehicle (position, velocity, acceleration, and attitude).



Aircraft Trajectory relative to ground reference gid.

The new georegistration approach was validated by computer simulation based on an aircraft flying at a speed of 70 m/s in a 3-km radius circle at an altitude of 15,000 ft ($\approx 4,600$ m), using a camera pointed at the ground toward the center of the circle. Results from

using the nonlinear estimation algorithm, in combination with GPS and camera images taken once per second, indicate that after 20 minutes of operation, real-time georegistration errors are reduced to values of less than 2 m, 1 sigma, on the ground.

The new method is very modular and cleanly separates computer vision functions from optimal estimation functions. This allows the vision and estimation functions to be developed separately, and leverages the power of modern estimation theory to fuse information in an optimal manner. Heuristics are avoided, which are generally suboptimal, as are other methods that require human-in-the-loop intervention, ad hoc parameter weightings, and awkward stitching together of various types of data.

The work is applicable to any scientific or engineering application that requires finding the geolocation of specific objects seen in a sequence of camera images. For example, in a surveying application, the precise location and height of a mountain peak can be determined by having an airplane take aerial images while circling around it.

This work was done by David S. Bayard and Curtis W. Padgett of Caltech for NASA's Jet Propulsion Laboratory. Further information is contained in a TSP (see page 1).

This software is available for commercial licensing. Please contact Daniel Broderick of the California Institute of Technology at danielb@caltech.edu. Refer to NPO-47255.

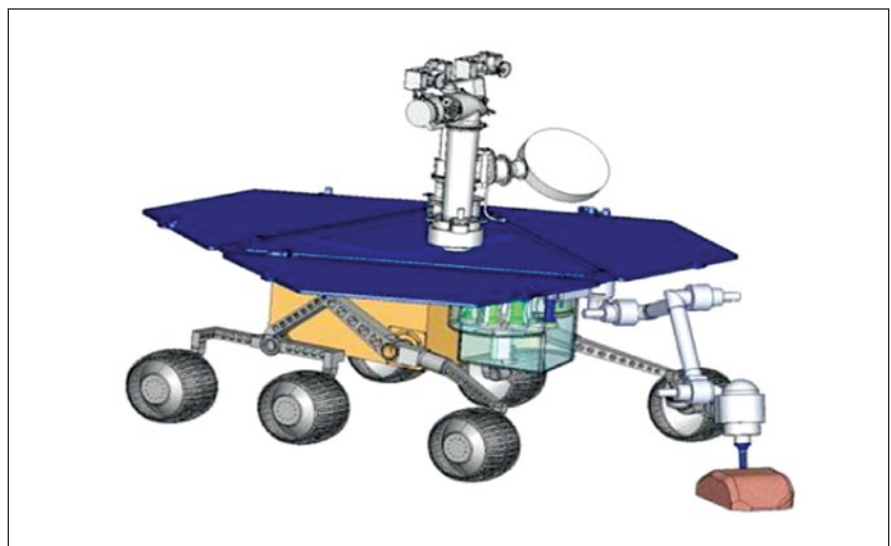
⚙️ Optimal Force Control of Vibro-Impact Systems for Autonomous Drilling Applications

A method is investigated how to maximize energy transfer to tools used in drilling, and can be applied to regular power tools.

NASA's Jet Propulsion Laboratory, Pasadena, California

The need to maintain optimal energy efficiency is critical during the drilling operations performed on future and current planetary rover missions (see figure). Specifically, this innovation seeks to solve the following problem. Given a spring-loaded percussive drill driven by a voice-coil motor, one needs to determine the optimal input voltage waveform (periodic function) and the optimal hammering period that minimizes the dissipated energy, while ensuring that the hammer-to-rock impacts are made with sufficient (user-defined) impact velocity (or impact energy).

To solve this problem, it was first observed that when voice-coil-actuated percussive drills are driven at high power, it is of paramount importance to ensure that the electrical current of the device remains in phase with the velocity of the



Planetary Rover equipped with a rotary percussive drill.

hammer. Otherwise, negative work is performed and the drill experiences a loss of performance (i.e., reduced impact energy) and an increase in Joule heating (i.e., reduction in energy efficiency). This observation has motivated many drilling products to incorporate the standard bang-bang control approach for driving their percussive drills. However, the bang-bang control approach is significantly less efficient than the optimal energy-efficient control approach solved herein.

To obtain this solution, the standard tools of classical optimal control theory were applied. It is worth noting that these tools inherently require the solution of a two-point boundary value problem

(TPBVP), i.e., a system of differential equations where half the equations have unknown boundary conditions. Typically, the TPBVP is impossible to solve analytically for high-dimensional dynamic systems. However, for the case of the spring-loaded vibro-impactor, this approach yields the exact optimal control solution as the sum of four analytic functions whose coefficients are determined using a simple, easy-to-implement algorithm. Once the optimal control waveform is determined, it can be used optimally in the context of both open-loop and closed-loop control modes (using standard real-time control hardware).

Future NASA *in situ* exploration missions increasingly require extensive

drilling and coring procedures that stress the demand for more energy efficient methods to accomplish these tasks. For example, when rover-based autonomous drills are controlled non-optimally for long periods of time, the energy loss can grow at a rate that cannot be sustained by the rover's internal energy supply. Motorized percussive units can be especially energy-draining (when controlled non-optimally), making this technology especially relevant to this type of future NASA work.

This work was done by Jack B. Aldrich and Avi B. Okon of Caltech for NASA's Jet Propulsion Laboratory. Further information is contained in a TSP (see page 1). NPO-48467

Low-Cost Telemetry System for Small/Micro Satellites

Marshall Space Flight Center, Alabama

A Software Defined Radio (SDR) concept uses a minimum amount of analog/radio frequency components to up/downconvert the RF signal to/from a digital format. Once in the digital domain, all other processing (filtering, modulation, demodulation, etc.) is done in software. The project will leverage existing designs and enhance capabilities in the commercial sector to provide a path to a radiation-hardened SDR transponder.

The SDR transponder would incorporate baseline technologies dealing with improved Forward Error Correcting (FEC) codes to be deployed to all Near Earth Network (NEN) ground stations.

By incorporating this FEC, at least a tenfold increase in data throughput can be achieved.

A family of transponder products can be implemented using common platform architecture, allowing new products to be more quickly introduced into the market. Software can be reused across products, reducing software/hardware costs dramatically. New features and capabilities, such as encoding and decoding algorithms, filters, and bit synchronizers, can be added to the existing infrastructure without requiring major new capital expenditures, allowing implementation of advanced features in the communication systems.

As new telecommunication technologies emerge, incorporating them into the SDR fabric will be easily accomplished with little or no requirements for new hardware. There are no preferred flight platforms for the SDR technology, so it can be used on any type of orbital or sub-orbital platform, all within a fully radiation hardened design.

This work was done by William Sims and Kosta Varnavas of Marshall Space Flight Center.

This invention is owned by NASA, and a patent application has been filed. For further information, contact Sammy Nabors, MSFC Commercialization Assistance Lead, at sammy.a.nabors@nasa.gov. Refer to MFS-32871-1.

Operator Interface and Control Software for the Reconfigurable Surface System Tri-ATHLETE

The capability of future exploration missions may be greatly extended for a small additional cost.

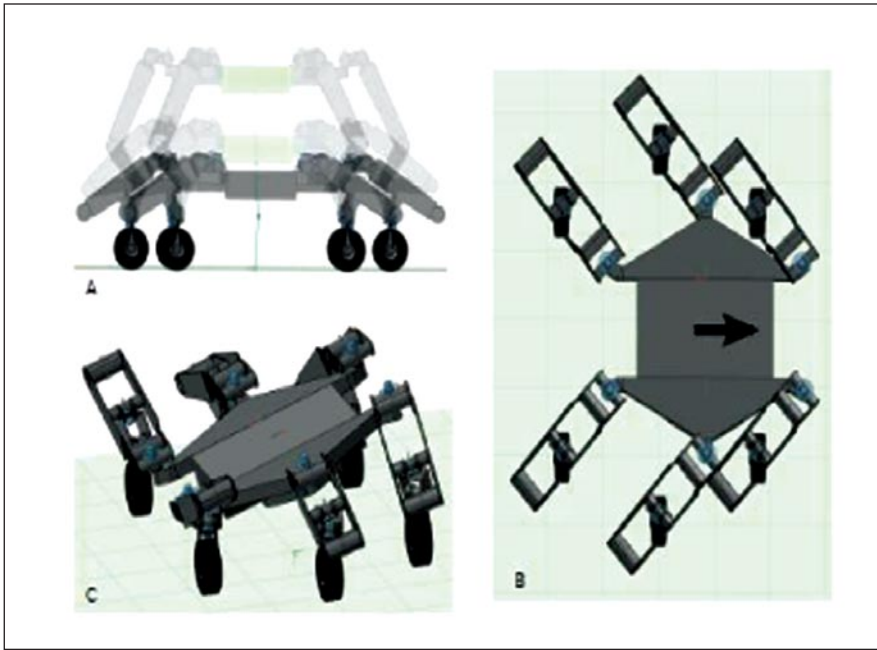
NASA's Jet Propulsion Laboratory, Pasadena, California

Graphical operator interface methods have been developed for modular, reconfigurable articulated surface systems in general, and a specific instantiation thereof for JPL's Tri-ATHLETE. The All-Terrain Hex-Limbed Extra-Terrestrial Explorer Robot (ATHLETE) has six limbs with six kinematic degrees of freedom each (see figure).

The core advancement of this work was the development of a novel set of algorithms for dynamically maintaining a reduced coordinate model of any connected assembly of robot modules. The kinematics of individual modules are first modeled using a catalog of 12 standard 3D robot joints (this modeling step needs to be done only once). Then, in-

dividual modules can be assembled into any closed- or open-chain topology. The system automatically maintains a spanning tree of the overall configuration, which ensures both efficiency and accuracy of the on-screen representation.

Until now, JPL has used generic CAD (computer-aided design), simulation, and animation tools as a substitute for a



Any **Assembly of Kinematic Modules** may be directly operated in the system by click-and-drag direct manipulation. Here the canonical configuration of two Tri-ATHLETE modules and one pallet is operated in lifting (A), sliding (B), and tilting (C) motions.

true modular robot operator interface. This workflow is extremely time-consuming, and is not suited for use in an operations context. Current operator interfaces, both at JPL and in the

broader exploration robotics community, are largely focused on non-reconfigurable hardware.

Reconfigurable modular hardware such as Tri-ATHLETE promises to ex-

tend greatly the capability of future exploration missions for a relatively small additional cost. Whereas existing missions based on monolithic hardware can only perform a limited set of pre-defined operations, modular hardware can potentially be reconnected and recombined to serve a range of functions. The full realization of these promises is contingent not just on the development of the hardware itself, but also upon the availability of corresponding software systems with algorithms that enable operators to rapidly specify, visualize, simulate, and control particular assemblies of modules. In the case of articulated, reconnectable hardware like Tri-ATHLETE, operators also can determine feasible motions of the assembly, and disconnect/reconnect actions that change assembly topology.

This work was done by Jeffrey S. Norris of Caltech, Marsette A. Vona of Northeastern University, and Daniela Rus of MIT for NASA's Jet Propulsion Laboratory. Further information is contained in a TSP (see page 1).

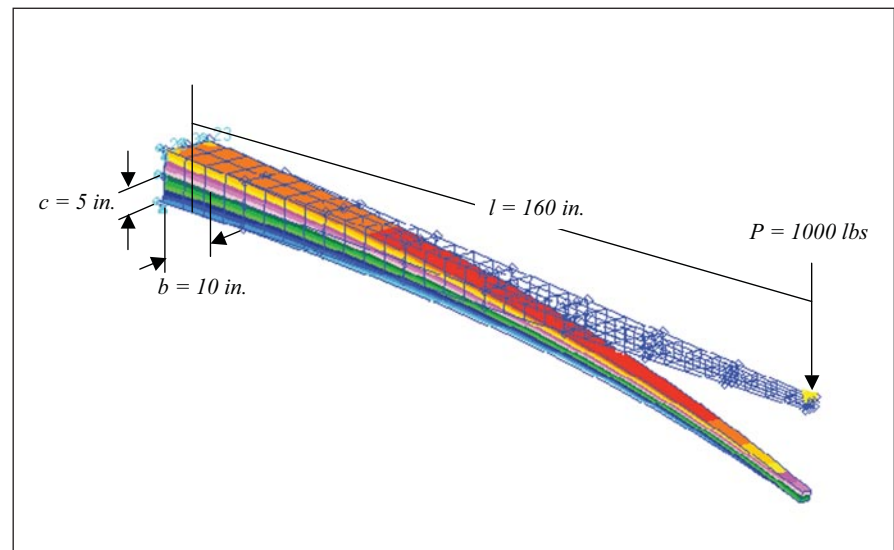
This software is available for commercial licensing. Please contact Daniel Broderick of the California Institute of Technology at danielb@caltech.edu. Refer to NPO-47777.

▶ Algorithms for Determining Physical Responses of Structures Under Load

Structure can be monitored in real time while in actual service.

Dryden Flight Research Center, Edwards, California

Ultra-efficient real-time structural monitoring algorithms have been developed to provide extensive information about the physical response of structures under load. These algorithms are driven by actual strain data to measure accurately local strains at multiple locations on the surface of a structure. Through a single point load calibration test, these structural strains are then used to calculate key physical properties of the structure at each measurement location. Such properties include the structure's flexural rigidity (the product of the structure's modulus of elasticity, and its moment of inertia) and the section modulus (the moment of inertia divided by the structure's half-depth). The resulting structural properties at each location can be used to determine the structure's bending moment, shear, and



Cantilever Beam of tapered cross section subjected to tip loading.

structural loads in real time while the structure is in service.

The amount of structural information can be maximized through the use of highly multiplexed fiber Bragg grating technology using optical time domain reflectometry and optical frequency domain reflectometry, which can provide a local strain measurement every 10 mm on a single hair-sized optical fiber. Since local strain is used as input to the algorithms, this system

serves multiple purposes of measuring strains and displacements, as well as determining structural bending moment, shear, and loads for assessing real-time structural health.

The first step is to install a series of strain sensors on the structure's surface in such a way as to measure bending strains at desired locations. The next step is to perform a simple ground test calibration. For a beam of length l (see example), discretized into n sections

and subjected to a tip load of P that places the beam in bending, the flexural rigidity of the beam can be experimentally determined at each measurement location x . The bending moment at each station can then be determined for any general set of loads applied during operation.

This work was done by W. Lance Richards and William L. Ko of Dryden Flight Research Center. Further information is contained in a TSP (see page 1). DRC-008-023

Mission Analysis, Operations, and Navigation Toolkit Environment (Monte) Version 040

NASA's Jet Propulsion Laboratory, Pasadena, California

Monte is a software set designed for use in mission design and spacecraft navigation operations. The system can process measurement data, design optimal trajectories and maneuvers, and do orbit determination, all in one application. For the first time, a single software set can be used for mission design and navigation operations. This eliminates problems due to different models and fidelities used in legacy mission design and navigation software.

The unique features of Monte 040 include a blowdown thruster model for GRAIL (Gravity Recovery and Interior Laboratory) with associated pressure models, as well as an updated, optimal-search capability (COSMIC) that facilitated mission design for ARTEMIS. Existing legacy software lacked the capabilities necessary for these two missions. There is also a mean orbital element propagator and an osculating to mean element converter that allows long-term orbital stability analysis for the first time in compiled code.

The optimized trajectory search tool COSMIC allows users to place constraints and controls on their searches without any restrictions. Constraints may be user-defined and depend on trajectory information either forward or backwards in time. In addition, a long-term orbit stability analysis tool (morbiter) existed previously as a set of scripts on top of Monte.

Monte is becoming the primary tool for navigation operations, a core competency at JPL. The mission design capabilities in Monte are becoming mature enough for use in project proposals as well as post-phase A mission design.

Monte has three distinct advantages over existing software. First, it is being

developed in a modern paradigm: object-oriented C++ and Python. Second, the software has been developed as a toolkit, which allows users to customize their own applications and allows the development team to implement requirements quickly, efficiently, and with minimal bugs. Finally, the software is managed in accordance with the CMMI (Capability Maturity Model Integration), where it has been appraised at maturity level 3.

This work was done by Richard F. Sunseri, Hsi-Cheng Wu, Scott E. Evans, James R. Evans, Theodore R. Drain, and Michelle M. Guevara of Caltech for NASA's Jet Propulsion Laboratory.

This software is available for commercial licensing. Please contact Daniel Broderick of the California Institute of Technology at danielb@caltech.edu. Refer to NPO-48184.

Autonomous Rover Traverse and Precise Arm Placement on Remotely Designated Targets

NASA's Jet Propulsion Laboratory, Pasadena, California

This software controls a rover platform to traverse rocky terrain autonomously, plan paths, and avoid obstacles using its stereo hazard and navigation cameras. It does so while continuously tracking a target of interest selected from 10–20 m away. The rover drives and tracks the target until it reaches the vicinity of the target. The rover then positions itself to approach the target, deploys its robotic arm, and places the end effector in-

strument on the designated target to within 2–3-cm accuracy of the originally selected target.

This software features continuous navigation in a fairly rocky field in an outdoor environment and the ability to enable the rover to avoid large rocks and traverse over smaller ones. Using point-and-click mouse commands, a scientist designates targets in the initial imagery acquired from the rover's mast cameras. The navigation software uses

stereo imaging, traversability analysis, path planning, trajectory generation, and trajectory execution. It also includes visual target tracking of a designated target selected from 10 m away while continuously navigating the rocky terrain.

Improvements in this design include steering while driving, which uses continuous curvature paths. There are also several improvements to the traversability analyzer, including improved data fu-

sion of traversability maps that result from pose estimation uncertainties, dealing with boundary effects to enable tighter maneuvers, and handling a wider range of obstacles.

This work advances what has been previously developed and integrated on the Mars Exploration Rovers by using algorithms that are capable of traversing more rock-dense terrains,

enabling tight, thread-the-needle maneuvers. These algorithms were integrated on the newly refurbished Athena Mars research rover, and were fielded in the JPL Mars Yard. Forty-three runs were conducted with targets at distances ranging from 5 to 15 m, and a success rate of 93% was achieved for placement of the instrument within 2–3 cm of the target.

This work was done by Issa A. Nesnas and Mihail N. Pivtoraiko of Caltech, Alonzo Kelly of Carnegie Mellon University, and Michael Fleder of MIT for NASA's Jet Propulsion Laboratory. Further information is contained in a TSP (see page 1).

This software is available for commercial licensing. Please contact Daniel Broderick of the California Institute of Technology at danielb@caltech.edu. Refer to NPO-48062.

Computing Radiative Transfer in a 3D Medium

NASA's Jet Propulsion Laboratory, Pasadena, California

A package of software computes the time-dependent propagation of a narrow laser beam in an arbitrary three-dimensional (3D) medium with absorption and scattering, using the transient-discrete-ordinates method and a direct integration method. Unlike prior software that utilizes a Monte Carlo method, this software enables simulation at very small signal-to-noise ratios. The ability to simulate propagation of a narrow laser beam in a 3D medium is an improvement over other discrete-ordinate software. Unlike other direct

integration software, this software is not limited to simulation of propagation of thermal radiation with broad angular spread in three dimensions or of a laser pulse with narrow angular spread in two dimensions. Uses for this software include (1) computing scattering of a pulsed laser beam on a material having given elastic scattering and absorption profiles, and (2) evaluating concepts for laser-based instruments for sensing oceanic turbulence and related measurements of oceanic mixed-layer depths. With suitable augmentation, this soft-

ware could be used to compute radiative transfer in ultrasound imaging in biological tissues, radiative transfer in the upper Earth crust for oil exploration, and propagation of laser pulses in telecommunication applications.

This program was written by Paul Von Allmen and Seungwon Lee of Caltech for NASA's Jet Propulsion Laboratory. For more information, contact iaoffice@jpl.nasa.gov.

This software is available for commercial licensing. Please contact Daniel Broderick of the California Institute of Technology at danielb@caltech.edu. Refer to NPO-44719.

Architectural Implementation of NASA Space Telecommunications Radio System Specification

NASA's Jet Propulsion Laboratory, Pasadena, California

This software demonstrates a working implementation of the NASA STRS (Space Telecommunications Radio System) architecture specification. This is a developing specification of software architecture and required interfaces to provide commonality among future NASA and commercial software-defined radios for space, and allow for easier mixing of software and hardware from different vendors.

It provides required functions, and supports interaction with STRS-compliant simple test plug-ins (“waveforms”). All of it is programmed in “plain C,” except where necessary to interact with C++ plug-ins. It offers a small footprint, suitable for use in JPL radio hardware.

Future NASA work is expected to develop into fully capable software-defined radios for use on the space station, other

space vehicles, and interplanetary probes.

This work was done by Kenneth J. Peters, James P. Lux, Minh Lang, and Courtney B. Duncan of Caltech for NASA's Jet Propulsion Laboratory. Further information is contained in a TSP (see page 1).

This software is available for commercial licensing. Please contact Daniel Broderick of the California Institute of Technology at danielb@caltech.edu. Refer to NPO-47328.

Journal and Wave Bearing Impedance Calculation Software

John H. Glenn Research Center, Cleveland, Ohio

The wave bearing software suite is a MALTA application that computes bearing properties for user-specified wave bearing conditions, as well as plain journal bearings. Wave bearings are fluid

film journal bearings with multi-lobed wave patterns around the circumference of the bearing surface. In this software suite, the dynamic coefficients are outputted in a way for easy implementation

in a finite element model used in rotor dynamics analysis. The software has a graphical user interface (GUI) for inputting bearing geometry parameters, and uses MATLAB's structure interface

for ease of interpreting data. This innovation was developed to provide the stiffness and damping components of wave bearing impedances.

The computational method for computing bearing coefficients was originally designed for plain journal bearings and tilting pad bearings. Modifications to include a wave bearing profile consisted of changing the film thickness

profile given by an equation, and writing an algorithm to locate the integration limits for each fluid region. Careful consideration was needed to implement the correct integration limits while computing the dynamic coefficients, depending on the form of the input/output variables specified in the algorithm.

This work was done by Amanda Hanford and Robert Campbell of ARL/Penn State for

Glenn Research Center. For further information, contact the GRC Innovation Partnerships Office at (216) 433-8047.

Inquiries concerning rights for the commercial use of this invention should be addressed to NASA Glenn Research Center, Innovative Partnerships Office, Attn: Steven Fedor, Mail Stop 4-8, 21000 Brookpark Road, Cleveland, Ohio 44135. Refer to LEW-18627-1.

Scalable Integrated Multi-Mission Support System (SIMSS) Simulator Release 2.0 for GMSEC

Goddard Space Flight Center, Greenbelt, Maryland

Scalable Integrated Multi-Mission Support System (SIMSS) Simulator Release 2.0 software is designed to perform a variety of test activities related to spacecraft simulations and ground segment checks. This innovation uses the existing SIMSS framework, which interfaces with the GMSEC (Goddard Mission Services Evolution Center) Application Programming Interface (API) Version 3.0 message middleware, and allows SIMSS to accept GMSEC stan-

dard messages via the GMSEC message bus service.

SIMSS is a distributed, component-based, plug-and-play client-server system that is useful for performing real-time monitoring and communications testing. SIMSS runs on one or more workstations, and is designed to be user-configurable, or to use predefined configurations for routine operations. SIMSS consists of more than 100 modules that can be configured to create, receive,

process, and/or transmit data. The SIMSS/GMSEC innovation is intended to provide missions with a low-cost solution for implementing their ground systems, as well as to significantly reduce a mission's integration time and risk.

This work was done by John Kim, Sarma Velamuri, Taylor Casey, and Travis Bemann of Honeywell Technology Solutions, Inc. for Goddard Space Flight Center. For further information, contact the Goddard Innovative Partnerships Office at (301) 286-5810. GSC-16039-1

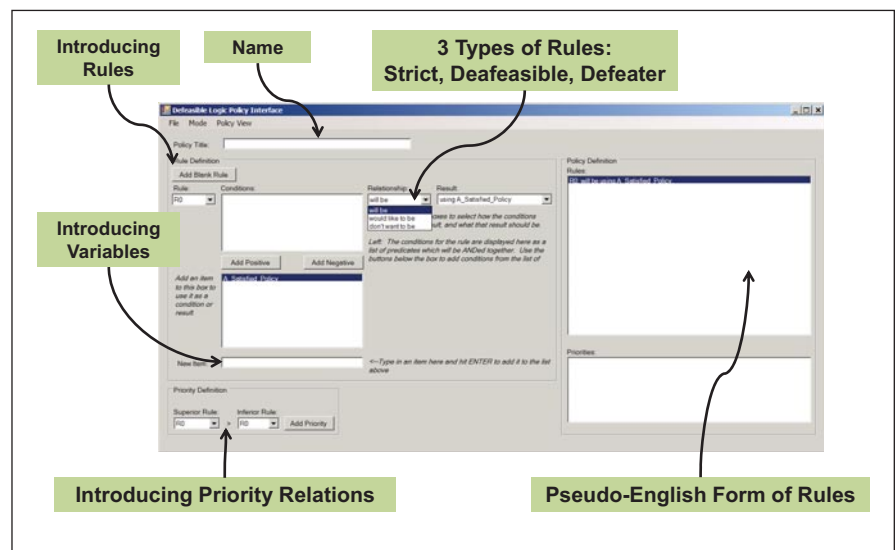
Policy-Based Negotiation Engine for Cross-Domain Interoperability

This method can be used by any organization with distributed Web entities.

NASA's Jet Propulsion Laboratory, Pasadena, California

A successful policy negotiation scheme for Policy-Based Management (PBM) has been implemented. Policy negotiation is the process of determining the "best" communication policy that all of the parties involved can agree on. Specifically, the problem is how to reconcile the various (and possibly conflicting) communication protocols used by different divisions. The solution must use protocols available to all parties involved, and should attempt to do so in the best way possible. Which protocols are commonly available, and what the definition of "best" is will be dependent on the parties involved and their individual communications priorities.

This method is based on defeasible policy composition (DPC), a new approach for finding conflicts and resolv-



Defeasible Logic Policy Editor

ing priorities between rules. A formulation and scenario for how cross-domain interoperability can be achieved have been developed based on a negotiation mechanism between different parties (domains) so that all parties can agree on procedures for interacting with each other. An implementation of this methodology has been developed in the form of an executable code and corresponding GUI interface.

The network management and Web communication software used by the different organizations presents a stumbling block. Many of the tools used by the various divisions do not have the ability to communicate network management data with each other. At best, this means that manual human intervention into the communication protocols used at various network routers and endpoints is required. This process is tedious, error-prone, and slow.

The present methods have inherent inefficiency and are not fully automatic, which heavily restricts their practical applications. The new method is based on an efficient algorithm. The new engine utilizes defeasible logic to describe communication policy constraints and priorities. Defeasible logic (see figure) is non-monotonic, and contains three different types of rules: strict rules, which are strict “if/then” statements; defeasible rules that are “if this, then probably that” statements; and defeater rules that contradict the outcomes of defeasible rules.

The policy negotiation program reads in two files specifying the policies that the user wishes to combine, and outputs a single file describing the means of communication that satisfy both input policies, if any can be found.

To implement this method, a tool called DPC (Defeasible Policy Composition) was developed. To maintain

that efficiency in the DPC tool, the data structures for the individual terms of each constraint are joined in linked-list fashion to their constraints and to a parent object representing each term. This can be visualized as a linked grid, where the heads of each column are the terms, the heads of each row are the rule names, and the body of the grid is the references to the terms that make up those rules. Each term reference is linked to its neighbors in the grid, which allows the algorithm to quickly and efficiently search through, add, and delete rows, terms, and individual term references.

This work was done by Farrokh Vatan and Edward T. Chow of Caltech for NASA's Jet Propulsion Laboratory. Further information is contained in a TSP (see page 1).

The software used in this innovation is available for commercial licensing. Please contact Daniel Broderick of the California Institute of Technology at danielb@caltech.edu. Refer to NPO-48399.

Linked-List-Based Multibody Dynamics (MBDyn) Engine

Lyndon B. Johnson Space Center, Houston, Texas

This new release of MBDyn is a software engine that calculates the dynamics states of kinematic, rigid, or flexible multibody systems. An MBDyn multibody system may consist of multiple groups of articulated chains, trees, or closed-loop topologies. Transient topologies are handled through conservation of energy and momentum. The solution for rigid-body systems is exact, and several configurable levels of non-linear term fidelity are available for flexible dynamics systems.

The algorithms have been optimized for efficiency and can be used for both non-real-time (NRT) and real-time (RT) simulations. Interfaces are currently compatible with NASA's Trick Simulation Environment. This new release represents a significant advance in capability and ease of use. The two most significant new additions are an application programming interface (API) that clarifies and simplifies use of MBDyn, and a link-list infrastructure that allows a single MBDyn instance to propagate an

arbitrary number of interacting groups of multibody topologies.

MBDyn calculates state and state derivative vectors for integration using an external integration routine. A Trick-compatible interface is provided for initialization, data logging, integration, and input/output.

This work was done by John Maclean, Thomas Brain, Leslie Quioco, An Huynh, and Tushar Ghosh of Johnson Space Center. Further information is contained in a TSP (see page 1). MSC-24925-1

Multi-Mission Power Analysis Tool (MMPAT) Version 3

NASA's Jet Propulsion Laboratory, Pasadena, California

The Multi-Mission Power Analysis Tool (MMPAT) simulates a spacecraft power subsystem including the power source (solar array and/or radioisotope thermoelectric generator), bus-voltage control, secondary battery (lithium-ion or nickel-hydrogen), thermostatic heaters, and power-consuming equipment. It handles multiple mission types including heliocentric orbiters, planetary orbiters, and surface operations. Being parametrically

driven along with its user-programmable features can reduce or even eliminate any need for software modifications when configuring it for a particular spacecraft. It provides multiple levels of fidelity, thereby fulfilling the vast majority of a project's power simulation needs throughout the lifecycle. It can operate in a standalone mode with a graphical user interface, in batch mode, or as a library linked with other tools.

This software can simulate all major aspects of a spacecraft power subsystem. It is parametrically driven to reduce or eliminate the need for a programmer. Added flexibility is provided through user-designed state models and table-driven parameters.

MMPAT is designed to be used by a variety of users, such as power subsystem engineers for sizing power subsystem components; mission planners for

adjusting mission scenarios using power profiles generated by the model; system engineers for performing system-level trade studies using the results of the model during the early design phases of a spacecraft; and operations

personnel for high-fidelity modeling of the essential power aspect of the planning picture.

This work was done by Eric G. Wood, George W. Chang, and Fannie C. Chen of Caltech for NASA's Jet Propulsion Laboratory.

For more information, contact iaoffice@jpl.nasa.gov.

This software is available for commercial licensing. Please contact Daniel Broderick of the California Institute of Technology at danielb@caltech.edu. Refer to NPO-48152.

Jupiter Environment Tool

NASA's Jet Propulsion Laboratory, Pasadena, California

The Jupiter Environment Tool (JET) is a custom UI plug-in for STK that provides an interface to Jupiter environment models for visualization and analysis. Users can visualize the different magnetic field models of Jupiter through various rendering methods, which are fully integrated within STK's 3D Window. This allows users to take snapshots and make animations of their

scenarios with magnetic field visualizations. Analytical data can be accessed in the form of custom vectors. Given these custom vectors, users have access to magnetic field data in custom reports, graphs, access constraints, coverage analysis, and anywhere else vectors are used within STK.

This work was done by Erick J. Sturm, Kenneth M. Donahue, James P. Biehl, and

Michael Kokorowski of Caltech; Cedrick Ngalande of Microcosm, Inc.; and Jordan Boedecker of Iowa State University for NASA's Jet Propulsion Laboratory. Further information is contained in a TSP (see page 1).

This software is available for commercial licensing. Please contact Daniel Broderick of the California Institute of Technology at danielb@caltech.edu. Refer to NPO-47998.

Jet and Tropopause Products for Analysis and Characterization (JETPAC)

NASA's Jet Propulsion Laboratory, Pasadena, California

This suite of IDL programs provides identification and comprehensive characterization of the dynamical features of the jet streams in the upper troposphere, the lower stratospheric polar night jet, and the tropopause. The output of this software not only provides comprehensive information on the jets and tropopause, but also gives this information in a form that facilitates studies of observations in relation to the jets and tropopauses.

The programs use data from gridded meteorological analyses (including, currently, GEOS-5/MERRA and NCEP/GFS, but are designed to easily adapt to others) to identify the locations and char-

acteristics (wind speed, temperature, wind components, potential vorticity, equivalent latitude, potential temperature, relative vorticity, and other fields) at the jet maximum and the edges of the jet regions. It also compiles detailed tropopause information based on several commonly used definitions of the tropopause, including cataloging times/locations with multiple tropopauses. These products are calculated for the complete gridded meteorological datasets, and the differences between jet locations/characteristics and measurement locations/characteristics cataloged for several satellite (currently, Aura MLS, ACE, and HIRDLS) and aircraft (currently START-

08, Winter Storms, SPURT) datasets.

These products are currently being used in studies compiling jet and tropopause climatologies, and to characterize trace gas observations in relation to the jets and tropopauses. The output products will be made available to other collaborators, and eventually will be publicly available.

This work was done by Gloria L. Manney and William H. Daffer of Caltech for NASA's Jet Propulsion Laboratory. Further information is contained in a TSP (see page 1).

This software is available for commercial licensing. Please contact Daniel Broderick of the California Institute of Technology at danielb@caltech.edu. Refer to NPO-47709.

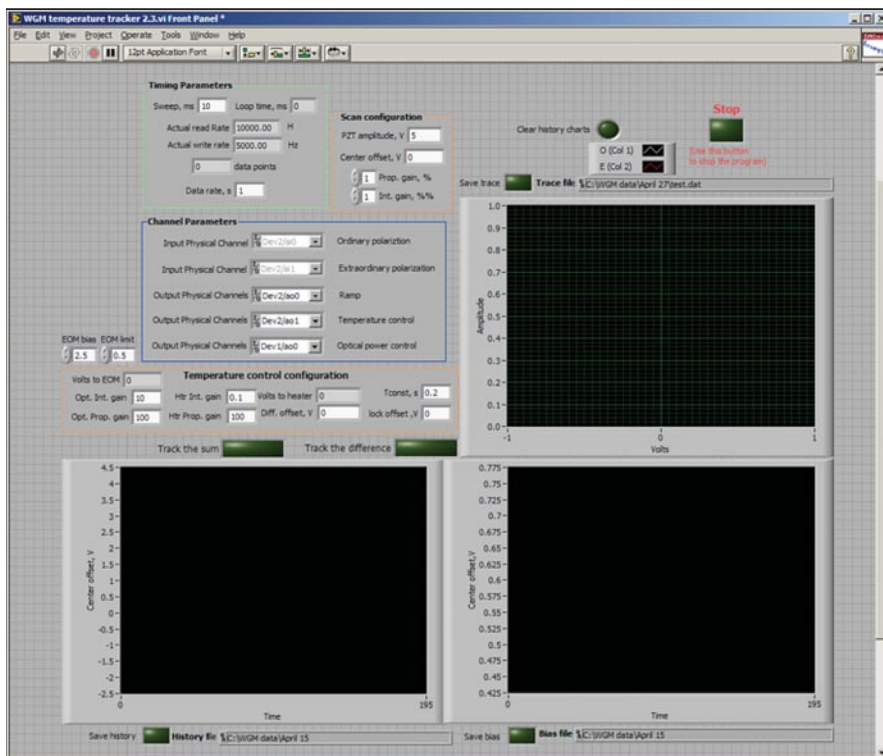
WGM Temperature Tracker

NASA's Jet Propulsion Laboratory, Pasadena, California

This software implements digital control of a WGM (whispering-gallery-mode) resonator temperature based on the dual-mode approach. It comprises one acquisition (dual-channel) and three control modules. The interaction of the proportional-integral

loops is designed in the original way, preventing the loops from fighting. The data processing is organized in parallel with the acquisition, which allows the computational overhead time to be suppressed or often completely avoided.

WGM resonators potentially provide excellent optical references for metrology, clocks, spectroscopy, and other applications. However, extremely accurate (below micro-Kelvin) temperature stabilization is required. This software allows one specifically advantageous



A Screen Shot of the WGM Temperature Tracker 2.3 graphic interface.

method of such stabilization to be implemented, which is immune to a variety of effects that mask the temperature variation.

WGM Temperature Tracker 2.3 (see figure) is a LabVIEW code developed for dual-mode temperature stabilization of WGM resonators. It has allowed for the temperature stabilization at the level of 200 nK with one-second integration time, and 6 nK with 10,000-second integration time, with the above room-temperature set point.

This software, in conjunction with the appropriate hardware, can be used as a noncryogenic temperature sensor/controller with sub-micro-Kelvin sensitivity, which at the time of this reporting considerably outperforms the state of the art.

This work was done by Dmitry V. Strekalov of Caltech for NASA's Jet Propulsion Laboratory. Further information is contained in a TSP (see page 1).

This software is available for commercial licensing. Please contact Daniel Broderick of the California Institute of Technology at danielb@caltech.edu. Refer to NPO-48306.

Large Terrain Continuous Level of Detail 3D Visualization Tool

NASA's Jet Propulsion Laboratory, Pasadena, California

This software solved the problem of displaying terrains that are usually too large to be displayed on standard workstations in real time. The software can visualize terrain data sets composed of billions of vertices, and can display these data sets at greater than 30 frames per second.

The Large Terrain Continuous Level of Detail 3D Visualization Tool allows

large terrains, which can be composed of billions of vertices, to be visualized in real time. It utilizes a continuous level of detail technique called clipmapping to support this. It offloads much of the work involved in breaking up the terrain into levels of details onto the GPU (graphics processing unit) for faster processing.

This work was done by Steven Myint and Abhinandan Jain of Caltech for NASA's Jet Propulsion Laboratory. For more information, contact iaoffice@jpl.nasa.gov.

This software is available for commercial licensing. Please contact Daniel Broderick of the California Institute of Technology at danielb@caltech.edu. Refer to NPO-47978.

SE-FIT

John H. Glenn Research Center, Cleveland, Ohio

The mathematical theory of capillary surfaces has developed steadily over the centuries, but it was not until the last few decades that new technologies have put a more urgent demand on a substantially more qualitative and quantitative understanding of phenomena relating to capillarity in general. So far, the new theory development successfully predicts the behavior of capillary surfaces for special cases. However, an efficient quantitative mathematical prediction of

capillary phenomena related to the shape and stability of geometrically complex equilibrium capillary surfaces remains a significant challenge. As one of many numerical tools, the open-source Surface Evolver (SE) algorithm has played an important role over the last two decades. The current effort was undertaken to provide a front-end to enhance the accessibility of SE for the purposes of design and analysis. Like SE, the new code is open-source and will remain

under development for the foreseeable future.

The ultimate goal of the current Surface Evolver – Fluid Interface Tool (SE-FIT) development is to build a fully integrated front-end with a set of graphical user interface (GUI) elements. Such a front-end enables the access to functionalities that are developed along with the GUIs to deal with pre-processing, convergence computation operation, and post-processing. In other words, SE-FIT

is not just a GUI front-end, but an integrated environment that can perform sophisticated computational tasks, e.g. importing industry standard file formats and employing parameter sweep functions, which are both lacking in SE, and require minimal interaction by the user. These functions are created using a mixture of Visual Basic and the SE script language. These form the foundation for a high-performance front-end that substantially simplifies use without sacrificing the proven capabilities of SE. The real power of SE-FIT lies in its automated pre-processing, pre-defined geometries, convergence computation operation, computational diagnostic tools, and crash-handling capabilities to sustain extensive computations.

SE-FIT performance is enabled by its so-called file-layer mechanism. During the early stages of SE-FIT development,

it became necessary to modify the original SE code to enable capabilities required for an enhanced and synchronized communication. To this end, a file-layer was created that serves as a command buffer to ensure a continuous and sequential execution of commands sent from the front-end to SE. It also establishes a proper means for handling crashes. The file layer logs input commands and SE output; it also supports user interruption requests, back and forward operation (i.e. 'undo' and 'redo'), and others. It especially enables the batch mode computation of a series of equilibrium surfaces and the searching of critical parameter values in studying the stability of capillary surfaces. In this way, the modified SE significantly extends the capabilities of the original SE.

There is a growing need for SE in subjects such as flows related to micrograv-

ity tankage, inkjet printing, nanotechnologies, transport in porous media, capillary self-assembly and self-alignment, microscale wicking structures, foams, and more. It is hoped that SE-FIT will prove to be an essential tool for myriad capillary design and analysis applications as well as a tool for both education and inquiry.

This work was done by Yongkang Chen, Mark Weislogel, Ben Schaeffer, Ben Semerjian, and Lihong Yang of the Portland State University Office of Research and Sponsored Projects; and Gregory Zimmerli of Glenn Research Center. Further information is contained in a TSP (see page 1).

Inquiries concerning rights for the commercial use of this invention should be addressed to NASA Glenn Research Center, Innovative Partnerships Office, Attn: Steven Fedor, Mail Stop 4-8, 21000 Brookpark Road, Cleveland, Ohio 44135. Refer to LEW-18824-1.

Scalable Integrated Multi-Mission Support System Simulator Release 3.0

Goddard Space Flight Center, Greenbelt, Maryland

The Scalable Integrated Multi-mission Support System (SIMSS) is a tool that performs a variety of test activities related to spacecraft simulations and ground segment checks.

The GSC Mission Services Evolution Center (GMSEC) has been advancing new technologies using its architecture to aid missions in the development of control centers, and to enable the interoperability of mission operations center (MOC) components. These new technologies are intended to provide missions with low-cost solutions in implementing their ground systems. SIMSS Version 2.0 was developed to run within the GMSEC architecture as a plug-in component. To accomplish this, SIMSS

is integrated with GMSEC application programming interface (API) 3.0 libraries, which allows SIMSS to successfully operate in the GMSEC environment and communicate with other components using GMSEC messages that are transmitted over the GMSEC messaging middleware interface bus.

This innovation (SIMSS Release 3.0) provides a Generic Simulator module, which supports the use of an XTCE-based project database (PDB) from which telemetry data is generated, and then is published onto the GMSEC message bus.

SIMSS is a distributed, component-based, plug-and-play client-server system useful for performing real-time monitor-

ing and communications testing. SIMSS runs on one or more workstations and is designed to be user-configurable or to use predefined configurations for routine operations. SIMSS consists of more than 100 modules that can be configured to create, receive, process, and/or transmit data. The SIMSS/GMSEC innovation is intended to provide missions with a low-cost solution for implementing their ground systems, as well as significantly reducing a mission's integration time and risk.

This work was done by John Kim, Sarma Velamuri, and Taylor Casey of Goddard Space Flight Center; and Travis Bemann of Honeywell. For further information, contact the Goddard Innovative Partnerships Office at (301) 286-5810. GSC-16041-1

Mars Express Forward Link Capabilities for the Mars Relay Operations Service (MaROS)

NASA's Jet Propulsion Laboratory, Pasadena, California

This software provides a new capability for landed Mars assets to perform forward link relay through the Mars Express (MEX) European Union orbital spacecraft. It solves the problem of stan-

dardizing the relay interface between lander missions and MEX.

The Mars Operations Relay Service (MaROS) is intended as a central point for relay planning and post-pass analysis

for all Mars landed and orbital assets. Through the first two phases of implementation, MaROS supports relay coordination through the Odyssey orbiter and the Mars Reconnaissance Orbiter (MRO).

With this new software, MaROS now fully integrates the Mars Express spacecraft into the relay picture. This new software generates and manages a new set of file formats that allows for relay request to MEX for forward and return link relay, including the parameters specific to MEX.

Existing MEX relay planning interactions were performed via email exchanges and point-to-point file transfers. By integrating MEX into MaROS, all transactions are managed by a central-

ized service for tracking and analysis. Additionally, all lander missions have a single, shared interface with MEX and do not have to integrate on a mission-by-mission basis.

Relay is a critical element of Mars lander data management. Landed assets depend largely upon orbital relay for data delivery, which can be impacted by the availability and health of each orbiter in the network. At any time, an issue may occur to prevent relay. For

this reason, it is imperative that all possible orbital assets be integrated into the overall relay picture.

This work was done by Daniel A. Allard, Michael N. Wallick, Roy E. Gladden, and Paul Wang of Caltech for NASA's Jet Propulsion Laboratory. Further information is contained in a TSP (see page 1).

This software is available for commercial licensing. Please contact Daniel Broderick of the California Institute of Technology at danielb@caltech.edu. Refer to NPO-48345.

▶ FERMI/GLAST Integrated Trending and Plotting System Release 5.0

Goddard Space Flight Center, Greenbelt, Maryland

An Integrated Trending and Plotting System (ITPS) is a trending, analysis, and plotting system used by space missions to determine performance and status of spacecraft and its instruments. ITPS supports several NASA mission operational control centers providing engineers, ground controllers, and scientists with access to the entire spacecraft telemetry data archive for the life of the mission, and includes a secure Web component for remote access.

FERMI/GLAST ITPS Release 5.0 features include the option to display dates (yyyy/dd) instead of orbit numbers along orbital Long-Term Trend (LTT) plot axis, the ability to save statistics from daily production plots as image files, and

removal of redundant "edit/create Input Definition File (IDF)" screens. Other features are a fix to address invalid packet lengths, a change in naming convention of image files in order to use in script, the ability to save all ITPS plot images (from Windows or the Web) as GIF or PNG format, the ability to specify y_{min} and y_{max} on plots where previously only the desired range could be specified, Web interface capability to plot IDFs that contain out-of-order page and plot numbers, and a fix to change all default file names to show yyyy-dddhhmmss time stamps instead of hh-mmssdddyyy.

A Web interface capability sorts files based on modification date (with newest one at top), and the statistics block can

be displayed via a Web interface. Via the Web, users can graphically view the volume of telemetry data from each day contained in the ITPS archive in the Web digest.

The ITPS could be also used in non-space fields that need to plot data or trend data, including financial and banking systems, aviation and transportation systems, healthcare and educational systems, sales and marketing, and housing and construction.

This work was done by Sheila Ritter of Goddard Space Flight Center, and Haim Bruner and Denise Reitan of Honeywell Technology Solutions. Further information is contained in a TSP (see page 1). GSC-15974-1

▶ Where's My Data — WMD

NASA's Jet Propulsion Laboratory, Pasadena, California

WMD provides a centralized interface to access data stored in the Mission Data Processing and Control System (MPCS) GDS (Ground Data Systems) databases during MSL (Mars Science Laboratory) Testbeds and ATLO (Assembly, Test, and Launch Operations) test sessions. The MSL project organizes its data based on venue (Testbed, ATLO, Ops), with each venue's data stored on a separate database, making it cumbersome for users to access data across the various venues.

WMD allows sessions to be retrieved through a Web-based search using several criteria: host name, session start date, or session ID number. Sessions matching

the search criteria will be displayed and users can then select a session to obtain and analyze the associated data.

The uniqueness of this software comes from its collection of data retrieval and analysis features provided through a single interface. This allows users to obtain their data and perform the necessary analysis without having to worry about where and how to get the data, which may be stored in various locations. Additionally, this software is a Web application that only requires a standard browser without additional plug-ins, providing a cross-platform, lightweight solution for users to retrieve and analyze their data.

This software solves the problem of efficiently and easily finding and retrieving data from thousands of MSL Testbed and ATLO sessions. WMD allows the user to retrieve their session in as little as one mouse click, and then to quickly retrieve additional data associated with the session.

This work was done by William L. Quach, Tadas Sesplaukis, Kyran J. Owen-Mankovich, and Lori L. Nakamura of Caltech for NASA's Jet Propulsion Laboratory. For more information, contact iaoffice@jpl.nasa.gov.

This software is available for commercial licensing. Please contact Daniel Broderick of the California Institute of Technology at danielb@caltech.edu. Refer to NPO-48362.

➤ Tiled WMS/KML Server V2

NASA's Jet Propulsion Laboratory, Pasadena, California

This software is a higher-performance implementation of tiled WMS, with integral support for KML and time-varying data. This software is compliant with the Open Geospatial WMS standard, and supports KML natively as a WMS return type, including support for the time attribute. Regionated KML wrappers are generated that match the existing tiled WMS dataset. Ping and JPG formats are supported, and the software is implemented as an Apache

2.0 module that supports a threading execution model that is capable of supporting very high request rates.

The module intercepts and responds to WMS requests that match certain patterns and returns the existing tiles. If a KML format that matches an existing pyramid and tile dataset is requested, regionated KML is generated and returned to the requesting application. In addition, KML requests that do not match the existing

tile datasets generate a KML response that includes the corresponding JPG WMS request, effectively adding KML support to a backing WMS server.

This work was done by Lucian Plesea of Caltech for NASA's Jet Propulsion Laboratory. For more information, contact iaoffice@jpl.nasa.gov.

This software is available for commercial licensing. Please contact Daniel Broderick of the California Institute of Technology at danielb@caltech.edu. Refer to NPO-47308.

➤ CometQuest: A Rosetta Adventure

NASA's Jet Propulsion Laboratory, Pasadena, California

CometQuest is an educational Apple iPhone game outlining the Rosetta mission to comet Churyumov-Gerasimenko. Its goal is to provide an enjoyable means to learn about the Rosetta mission through action gameplay where the player takes the role of Rosetta's mission operator and tries to capture and record as much science data as possible. It offers a multiple-choice quiz-type learning experience in which the player is asked to answer questions

about the Rosetta mission and comets in general. The answers to all the questions are included in the app's "Learn more" section.

CometQuest would become one of few NASA educational games available on the iPhone and iPad platforms, including the first educational NASA game optimized for iPad. The app is a specialized outreach tool for the Rosetta mission, enabling NASA to disseminate information and appreciation of its

value to the public in a medium otherwise unavailable.

This work was done by Nancy J. Leon, Diane K. Fisher, Alexander Novati, Artur B. Chmielewski, Austin J. Fitzpatrick, and Andrea Angram of Caltech for NASA's Jet Propulsion Laboratory. Further information is contained in a TSP (see page 1).

This software is available for commercial licensing. Please contact Daniel Broderick of the California Institute of Technology at danielb@caltech.edu. Refer to NPO-48582.

➤ Dig Hazard Assessment Using a Stereo Pair of Cameras

A lander can autonomously determine the areas within its robotic arm's workspace that have the least risk for digging hazards.

NASA's Jet Propulsion Laboratory, Pasadena, California

This software evaluates the terrain within reach of a lander's robotic arm for dig hazards using a stereo pair of cameras that are part of the lander's sensor system. A relative level of risk is calculated for a set of dig sectors. There are two versions of this software; one is designed to run onboard a lander as part of the flight software, and the other runs on a PC under Linux as a ground tool that produces the same results generated on the lander, given stereo images acquired by the lander and downlinked to Earth.

Onboard dig hazard assessment is accomplished by executing a workspace panorama command sequence. This sequence acquires a set of stereo pairs of images of the terrain the arm can reach, generates a set of candidate dig sectors,

and assesses the dig hazard of each candidate dig sector.

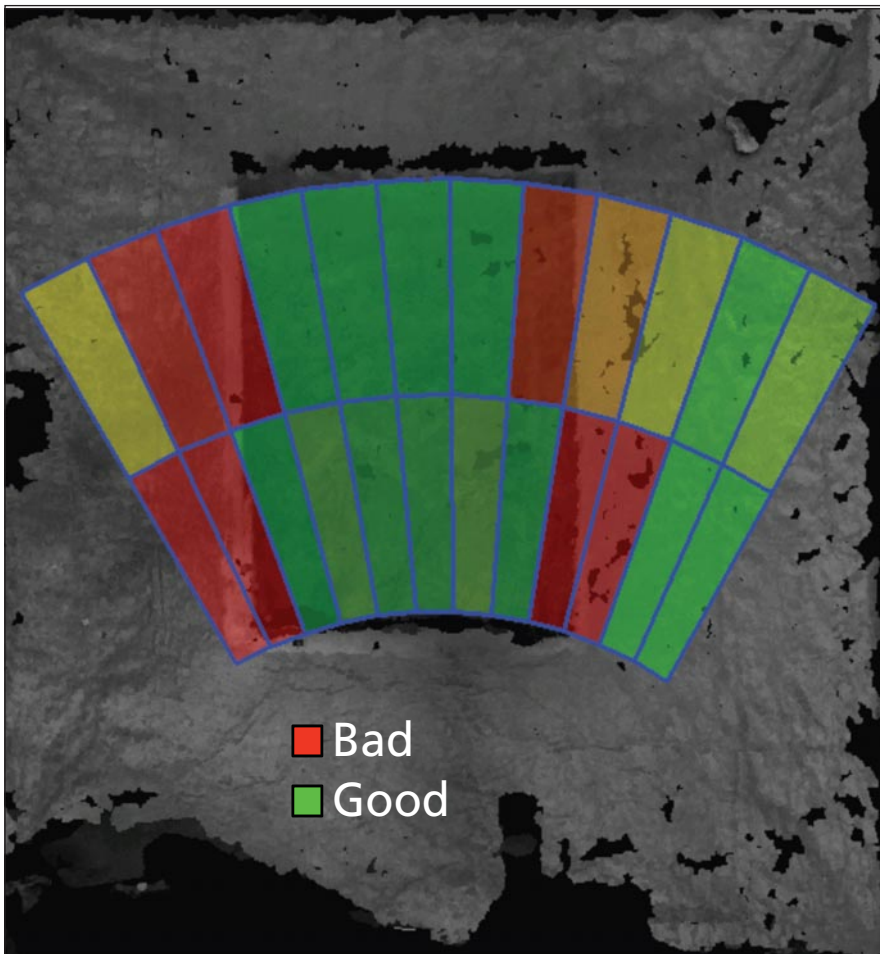
The 3D perimeter points of candidate dig sectors are generated using configurable parameters. A 3D reconstruction of the terrain in front of the lander is generated using a set of stereo images acquired from the mast cameras. The 3D reconstruction is used to evaluate the dig "goodness" of each candidate dig sector based on a set of eight metrics. The eight metrics are:

1. The maximum change in elevation in each sector,
2. The elevation standard deviation in each sector,
3. The forward tilt of each sector with respect to the payload frame,
4. The side tilt of each sector with respect to the payload frame,

5. The maximum size of missing data regions in each sector,
6. The percentage of a sector that has missing data,
7. The roughness of each sector, and
8. Monochrome intensity standard deviation of each sector.

Each of the eight metrics forms a goodness image layer where the goodness value of each sector ranges from 0 to 1. Goodness values of 0 and 1 correspond to high and low risk, respectively. For each dig sector, the eight goodness values are merged by selecting the lowest one. Including the merged goodness image layer, there are nine goodness image layers for each stereo pair of mast images.

There are three modes of operation for the ground tool version of the software:



Eight metrics are used to determine the **Dig Hazard** goodness map in which the dig sectors within the 3D reconstruction are color-coded. Green sectors are safe for digging. The colors between green and red correspond to the increasing level of risk.

1. View image, dig sector, and “digability” data products generated onboard the lander.
2. Given a set of raw images from a stereo pair of mast cameras, generate image, dig sector, and dig hazard products identical to what would be generated onboard the lander and view them.
3. Given a set of image products down-linked from the lander, generate dig sector and dig hazard products identical to what would be generated onboard the lander and view them. The ground tool can be used to view the 3D reconstruction of the terrain. The mouse buttons can be used to rotate the 3D model of the terrain and zoom in and out. Drop-down menus enable the user to display the dig sectors, one of the eight goodness image layers, and the merged goodness map layer. When viewing a goodness map layer, the dig sectors within the 3D reconstruction are color-coded. Green sectors are safe for digging. The colors between green and red correspond to the increasing level of risk.

This work was done by Arturo L. Rankin and Ashitey Trebi-Ollennu of Caltech for NASA’s Jet Propulsion Laboratory. Further information is contained in a TSP (see page 1).

The software used in this innovation is available for commercial licensing. Please contact Daniel Broderick of the California Institute of Technology at danielb@caltech.edu. Refer to NPO-48448.

High-Performance Modeling and Simulation of Anchoring in Granular Media for NEO Applications

NASA’s Jet Propulsion Laboratory, Pasadena, California

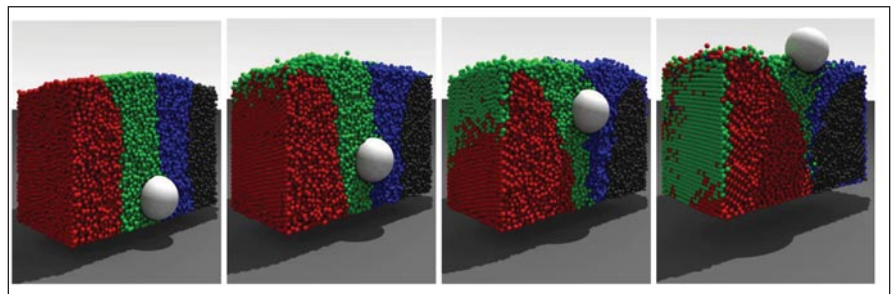
NASA is interested in designing a spacecraft capable of visiting a near-Earth object (NEO), performing experiments, and then returning safely. Certain periods of this mission would require the spacecraft to remain stationary relative to the NEO, in an environment characterized by very low gravity levels; such situations require an anchoring mechanism that is compact, easy to deploy, and upon mission completion, easy to remove.

The design philosophy used in this task relies on the simulation capability of a high-performance multibody dynamics physics engine. On Earth, it is difficult to create low-gravity conditions, and testing in low-gravity environments, whether artificial or in space, can be costly and very

difficult to achieve. Through simulation, the effect of gravity can be controlled with great accuracy, making it ideally suited to analyze the problem at hand.

Using Chrono::Engine, a simulation package capable of utilizing massively

parallel Graphic Processing Unit (GPU) hardware, several validation experiments were performed. Modeling of the regolith interaction has been carried out, after which the anchor penetration tests were performed and analyzed. The regolith



In this simulated **Brazil Nut Problem**, the large ball moves slowly up as the granular material is vibrated.

was modeled by a granular medium composed of very large numbers of convex three-dimensional rigid bodies, subject to microgravity levels and interacting with each other with contact, friction, and cohesive forces.

The multibody dynamics simulation approach used for simulating anchors penetrating a soil uses a differential variational inequality (DVI) methodology to solve the contact problem posed as a linear complementarity method (LCP). Implemented within a GPU processing

environment, collision detection is greatly accelerated compared to traditional CPU (central processing unit)-based collision detection. Hence, systems of millions of particles interacting with complex dynamic systems can be efficiently analyzed, and design recommendations can be made in a much shorter time. The figure shows an example of this capability where the Brazil Nut problem is simulated: as the container full of granular material is vibrated, the large ball slowly moves upwards. This capability

was expanded to account for anchors of different shapes and penetration velocities, interacting with granular soils.

This work was done by Marco B. Quadrelli and Abhinandan Jain of Caltech; and Dan Negrut and Hammad Mazhar of the University of Wisconsin-Madison for NASA's Jet Propulsion Laboratory. Further information is contained in a TSP (see page 1).

This software is available for commercial licensing. Please contact Daniel Broderick of the California Institute of Technology at danielb@caltech.edu. Refer to NPO-48332.

Mobile Multi-System Overview

NASA's Jet Propulsion Laboratory, Pasadena, California

At the time of this reporting, there are 2,589 rich mobile devices used at JPL, including 1,550 iPhones and 968 Blackberrys. Considering a total JPL population of 5,961 employees, mobile applications have a total addressable market of 43 percent of the employees at JPL, and that number is rising.

While it was found that no existing desktop tools can realistically be replaced by a mobile application, there is certainly a need to improve access to these desktop tools. When an alarm occurs and an engineer is away from his desk, a convenient

means of accessing relevant data can save an engineer a great deal of time and improve his job efficiency. To identify which data is relevant, an engineer benefits from a succinct overview of the data housed in 13+ tools. This need can be well met by a single, rich, mobile application that provides access to desired data across tools in the ops infrastructure.

This software is an iPhone app that allows a single configurable screen that presents an overview of many disparate Web applications. This tool can be applied to bring data from any public Web

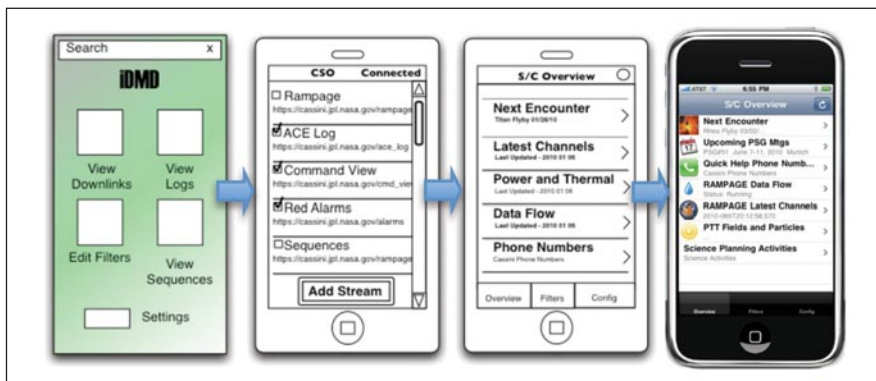
site into a native iPhone app. This concept (see figure) is similar to what the "Mint" financial aggregation site does to gather and format data from other Web sites, without APIs, onto its own site.

The benefits of this app are as follows:

- Developed as a native iPhone application, it thereby inherits iPhone usability and mobile device accessibility.
- Integration with seven distinct sources of data for the Cassini mission.
- Compatibility with existing html-based infrastructure, and requires no infrastructure upgrade.
- Configurable interface to show only relevant information to the user.
- Easily extendable to add information from any existing Web site.
- Does not intend to replace existing tools, only complement and increase user efficiency.

This work was done by Robert J. Witoff and David F. Doody of Caltech for NASA's Jet Propulsion Laboratory. Further information is contained in a TSP (see page 1).

This software is available for commercial licensing. Please contact Daniel Broderick of the California Institute of Technology at danielb@caltech.edu. Refer to NPO-47634.



User Interface Progression from concept to implementation.

Leveraging Cloud Computing to Improve Storage Durability, Availability, and Cost for MER Maestro

NASA's Jet Propulsion Laboratory, Pasadena, California

The Maestro for MER (Mars Exploration Rover) software is the premiere operation and activity planning software for the Mars rovers, and it is required to deliver all of the processed

image products to scientists on demand. These data span multiple storage arrays sized at 2 TB, and a backup scheme ensures data is not lost. In a catastrophe, these data would currently

recover at 20 GB/hour, taking several days for a restoration.

A seamless solution provides access to highly durable, highly available, scalable, and cost-effective storage capabilities.

This approach also employs a novel technique that enables storage of the majority of data on the cloud and some data locally. This feature is used to store the most recent data locally in order to guarantee utmost reliability in case of an outage or disconnect from the Internet. This also obviates any changes to the software that generates the most recent data set as it still has the same interface to the file system as it did before updates.

This software provides a seamless integration between existing software tools that would enable any mission across NASA to leverage the capability with minimal customization. It also unleashes a virtually limitless amount of storage and delivers it to projects without having to worry about provisioning, managing, and backing up large storage arrays.

The software integrates with Amazon Simple Storage Service (Amazon S3) service to provide the aforementioned

solutions. By integrating with S3, unprecedented durability is delivered to the storage system with 99.99999999% data retention rate. Furthermore, it is a self-healing replication system that repairs objects automatically if they are ever lost. Since data is stored on a per-object basis rather than a file system mount, correlated losses of objects are extremely unlikely and recovery of each object is fast. This also reduces reliance on a single file system, where an outage can take the system offline for extended duration. The solution, built on cloud computing technology, reduces MER Maestro's storage costs by over 80%. Most importantly, the solution is completely server-side, providing a seamless integration with existing clients without modifying any of their code or redelivering code.

An HTTP proxy was built that enables clients to access large amounts of data

on S3 securely, and without any changes to existing software. The proxy caches information and is capable of accessing data from local channels as well as on S3. This enables the proxy to serve the most recent data from local storage, while the older archived data is retrieved on-demand from S3. The data stored on S3 is private and can only be accessed by the proxy. Furthermore, the proxy authenticates its users through JPL LDAP, and verifies their membership in a specific group before giving them access to the data.

This work was done by George W. Chang, Mark W. Powell, John L. Callas, Recaredo J. Torres, and Khawaja S. Shams of Caltech for NASA's Jet Propulsion Laboratory. For more information, contact iaoffice@jpl.nasa.gov.

This software is available for commercial licensing. Please contact Daniel Broderick of the California Institute of Technology at danielb@caltech.edu. Refer to NPO-48189.

WMS Server 2.0

NASA's Jet Propulsion Laboratory, Pasadena, California

This software is a simple, yet flexible server of raster map products, compliant with the OGC WMS 1.1.1 protocol. The server is a full implementation of the OGC WMS 1.1.1 as a fastCGI client and using GDAL for data access. The server can operate in a proxy mode, where all or part of the WMS requests are done on a back server.

The server has explicit support for a colocated tiled WMS, including rapid response of black (no-data) requests. It generates JPEG and PNG images, in-

cluding 16-bit PNG. The GDAL backend support allows great flexibility on the data access.

The server is a port to a Linux/GDAL platform from the original IRIX/IL platform. It is simpler to configure and use, and depending on the storage format used, it has better performance than other available implementations.

The WMS server 2.0 is a high-performance WMS implementation due to the fastCGI architecture. The use of GDAL data back end allows for great

flexibility. The configuration is relatively simple, based on a single XML file. It provides scaling and cropping, as well as blending of multiple layers based on layer transparency.

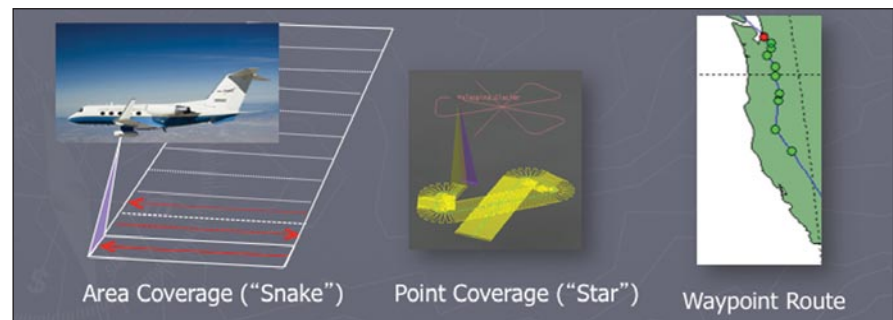
This work was done by Lucian Plesea and James F. Wood of Caltech for NASA's Jet Propulsion Laboratory. For more information, contact iaoffice@jpl.nasa.gov.

This software is available for commercial licensing. Please contact Daniel Broderick of the California Institute of Technology at danielb@caltech.edu. Refer to NPO-48330.

I-FORCAST: Rapid Flight Planning Tool

NASA's Jet Propulsion Laboratory, Pasadena, California

I-FORCAST (Instrument – Field of Regard Coverage Analysis and Simulation Tool) is a flight planning tool specifically designed for quickly verifying the feasibility and estimating the cost of airborne remote sensing campaigns (see figure). Flights are simulated by being broken into three predefined routing algorithms as necessary: mapping in a snaking pattern, mapping the area around a point target (like a volcano) with a star pattern, and mapping the area between a list of points.



Three Possible Scenarios were identified. This tool can handle all three as well as combinations.

The tool has been used to plan missions for radar, lidar, and in-situ atmospheric measuring instruments for a variety of aircraft. It has also been used for global and regional scale campaigns and automatically includes landings when refueling is required.

The software has been compared to the flight times of known commercial

aircraft route travel times, as well as a UAVSAR (Uninhabited Aerial Vehicle Synthetic Aperture Radar) campaign, and was within 15% of the actual flight time. Most of the discrepancy is due to non-optimal flight paths taken by actual aircraft to avoid restricted airspace and used to follow landing and take-off corridors.

This work was done by Bogdan Oaida, Mohammed O. Khan, and Michael B. Mercury of Caltech for NASA's Jet Propulsion Laboratory. Further information is contained in a TSP (see page 1).

This software is available for commercial licensing. Please contact Daniel Broderick of the California Institute of Technology at danielb@caltech.edu. Refer to NPO-48127.

Earth-Science Data Co-Locating Tool

NASA's Jet Propulsion Laboratory, Pasadena, California

This software is used to locate Earth-science satellite data and climate-model analysis outputs in space and time. This enables the direct comparison of any set of data with different spatial and temporal resolutions. It is written in three separate modules that are clearly separated for their functionality and interface with other modules. This enables a fast develop-

ment of supporting any new data set. In this updated version of the tool, several new front ends are developed for new products.

This software finds co-locatable data pairs for given sets of data products and creates new data products that share the same spatial and temporal coordinates. This facilitates the direct comparison between the two heterogeneous datasets

and the comprehensive and synergistic use of the datasets.

This work was done by Seungwon Lee, Lei Pan, and Gary L. Block of Caltech for NASA's Jet Propulsion Laboratory. Further information is contained in a TSP (see page 1).

This software is available for commercial licensing. Please contact Daniel Broderick of the California Institute of Technology at danielb@caltech.edu. Refer to NPO-48506.

Ascent/Descent Software

Lyndon B. Johnson Space Center, Houston, Texas

The Ascent/Descent Software Suite has been used to support a variety of NASA Shuttle Program mission planning and analysis activities, such as range safety, on the Integrated Planning System (IPS) platform. The Ascent/Descent Software Suite, containing Ascent Flight Design (ASC)/Descent Flight Design (DESC)

Configuration items (Cis), lifecycle documents, and data files used for shuttle ascent and entry modeling analysis and mission design, resides on IPS/Linux workstations. A list of tools in Navigation (NAV)/Prop Software Suite represents tool versions established during or after the IPS Equipment Rehost-3 project.

This work was done by Charles Brown, Robert Andrew, Scott Roe, Ronald Frye, Michael Harvey, Tuan Vu, Krishnaiyer Balachandran, and Ben Bly of the United Space Alliance for Johnson Space Center. For further information, contact the JSC Innovation Partnerships Office at (281) 483-3809. MSC-24960-1



National Aeronautics and
Space Administration